WYOMING STATE GEOLOGICAL SURVEY
Erin A. Campbell, Director and State Geologist
Laramie, Wyoming

Interpreting the past, providing for the future

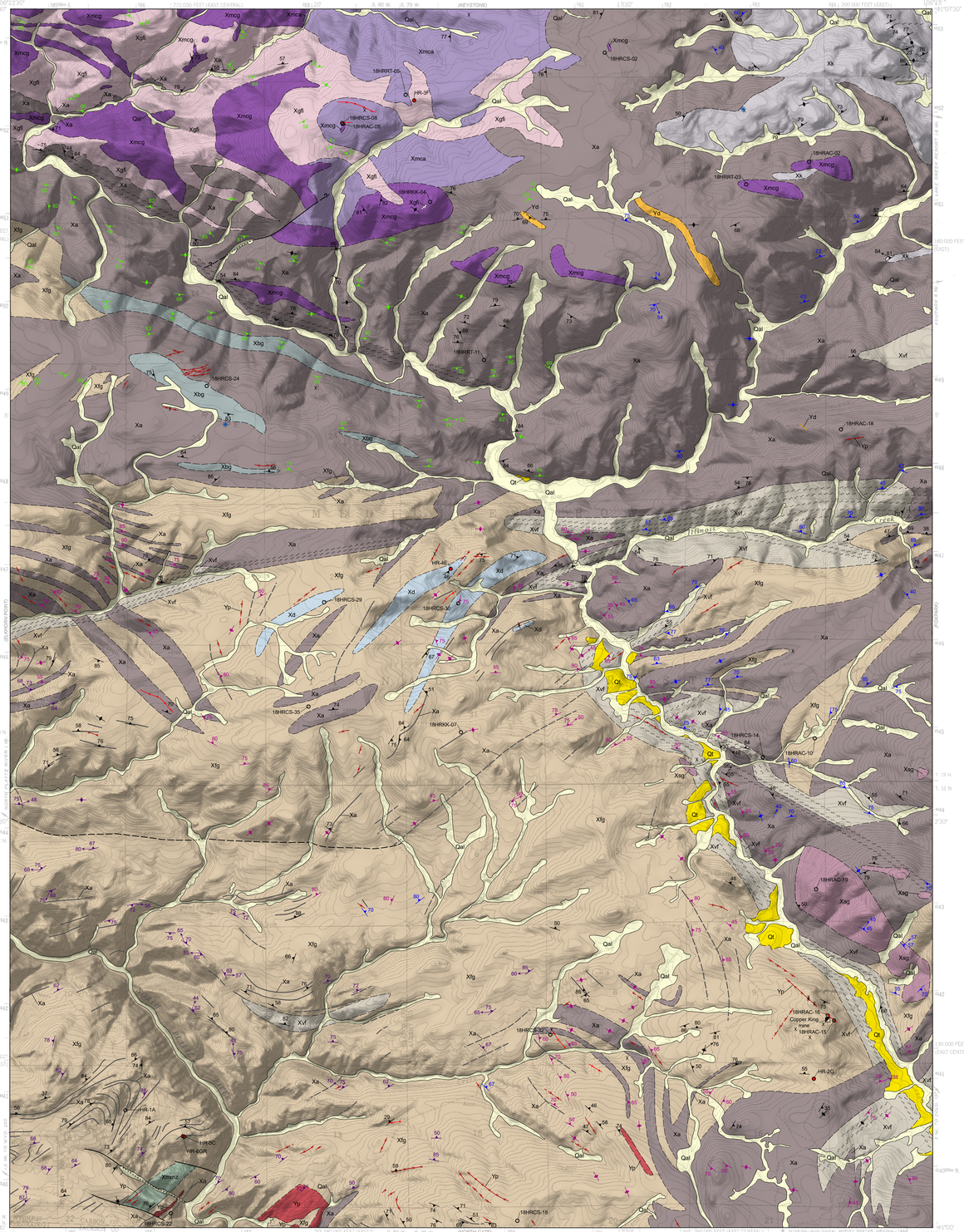

Base map from U.S. Geological Survey 1:24,000-scale topographic map of the Horatio Rock, Wyoming Quadrangle, 1961, photorevised 1983

Base hillshade derived from United States Elevation Data (NED) 10-meter Digital Elevation Model (DEM), 2006; azimuth 45°, sun angle 45°, vertical exaggeration 2.7

Projection: Universal Transverse Mercator (UTM), zone 13 North American Datum of 1927 (NAD 27)
1,000-meter grid ticks: UTM, zone 13
10,000-foot grid ticks: Wyoming State Plane Coordinate System, east and east central zones

Wyoming State Geological Survey
P.O. Box 1347 - Laramie, WY 82073-1347
Phone: 307-766-2286 - Fax: 307-766-2605
Email: wsgs-info@wyo.gov

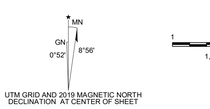

UTM GRID AND 2019 MAGNETIC NORTH DECLINATION AT CENTER OF SHEET

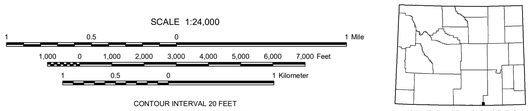

CONTOUR INTERVAL 20 FEET
NATIONAL GEODETIC VERTICAL DATUM OF 1929

WYOMING QUADRANGLE LOCATION

Digital cartography by Charles P. Samra, Adam S. Chumley, Rachel N. Toner, and Kelsey S. Kehoe

Map edited by Suzanne C. Luhr

Prepared in cooperation with and research supported by the U.S. Geological Survey, National Cooperative Geologic Mapping Program, under USGS award number G18AC00150. The views and conclusions contained in this document are those of the authors and should not be interpreted as necessarily representing the official policies, either expressed or implied, of the U.S. Government.

PRELIMINARY GEOLOGIC MAP OF THE HORATIO ROCK QUADRANGLE, ALBANY AND CARBON COUNTIES, WYOMING

by

Rachel N. Toner, Charles P. Samra, Adam S. Chumley, Kelsey S. Kehoe, and Andrea M. Loveland

2019

OPEN FILE REPORT 2019-5
Horatio Rock 1:24,000-scale Bedrock Geologic Map

EXPLANATION

CORRELATION OF MAP UNITS

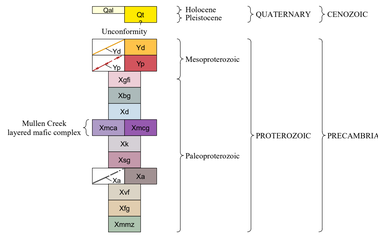

MAP SYMBOLS

Definitions: *Certain—Estimated location <25 m (82 ft)*
Approximate—Estimated location 25–100 m (82–330 ft)

Formation contact—Continuous where certain, long dash where approximate

Fault—Continuous where certain, long dash where approximate, dotted where concealed, queried where existence uncertain

Shear zone—Adapted from Ruehr (1961), Swetnam (1961), Houston and others (1968)

Granitic dike—Continuous where certain; see description of map units

Amphibolite dike—Continuous where certain, long dash where approximate, dotted where concealed; see description of map units

Pegmatite—Continuous where certain, long dash where approximate; see description of map units

Mineralized quartz vein

Carbonate breccia anomaly

Colored attitude symbols derived from:
Myers (1958)
Ruehr (1961)
Swetnam (1961)
Houston and others (1968)
This publication (OFR 2019-5)

Strike and dip of inclined foliation in igneous and metamorphic rocks

Strike of vertical foliation in igneous and metamorphic rocks

Bearing and plunge of lineation—May be combined with foliation symbol

Strike and dip of inclined mylonitic foliation

Strike and dip of inclined joint

Strike of vertical joint

Geochemistry sample—Showing sample name; sampled for whole rock geochemistry

Geochronology sample—Showing sample name; sampled for geochronology

Mine shaft, mostly collapsed or filled

Prospect pit

DESCRIPTION OF MAP UNITS

Cenozoic

Qal **Alluvial deposits (Holocene)**—Unconsolidated to poorly consolidated sand, silt, cobbles, gravel, and clay. May include colluvial, slope wash, and eluvial deposits. Material locally derived and present in and along ephemeral and permanent stream channels throughout the quadrangle. Maximum thickness approximately 8 m (26 ft)

Qt **Terrace deposits (Holocene–Pleistocene[?])**—Gravel, cobbles, sand, and silt deposits of mixed alluvial, colluvial, and eluvial origin approximately 3–5 m (10–16 ft) above the active floodplains of Pelton and Douglas creeks. Felsic gneiss, granite, and mafic rocks dominate the lithology in these deposits. Includes areas previously mapped as terrace gravels by Swetnam (1961). Thickness generally less than 3 m (10 ft)

Proterozoic

Yd **Granitic dike (Mesoproterozoic)**—Northwest–southeast-trending, orange to pink, fine- to medium-grained equigranular quartz- and potassium feldspar-rich granitic dikes. Contains magnetite and minor plagioclase, sphene, epidote, and biotite (McCallum and Houston, 1985). Dikes are undeformed and intrude into amphibolite units in the northeast portion of the quadrangle. Sutherland and Hausel (2004) associate these dikes with the Sherman Granite dated at 1,433±1.5 Ma by Frost and others (1999)

Yp **Pegmatite (Mesoproterozoic)**—White to pink to pale-orange, medium- to coarse-grained pegmatite composed primarily of potassium feldspar, quartz, and muscovite, with local occurrences of abundant small garnets. Commonly associated with bull quartz veins and prospect pits. This unit typically intrudes along host rock foliation, but occasionally crosscuts foliation or interfingers with and deforms host rocks. Contacts with mafic units are typically sharp, but gradational with felsic units. Outcrops located within shear zones may display brittle deformation. A pegmatite in the Woods Landing quadrangle to the east of the Horatio Rock quadrangle has a reported U-Pb age of 1,514±36 Ma (Campbell and Shelton, in press)

Xgfi **Granitic felsic intrusive (Mesoproterozoic–Paleoproterozoic)**—Gray to light-pink to light-orange, fine- to medium-grained granite and quartz monzonite, grading locally into a quartz-muscovite-microcline pegmatite. Mineral assemblages include potassium feldspar, quartz, and plagioclase, with local biotite and accessory epidote, garnet, and sphene. The unit crops out in the northwest portion of the quadrangle, specifically northwest of Douglas Creek, where it intrudes the Mullen Creek layered mafic complex. Unit foliation varies from unfoliated to moderately foliated near contacts with mafic units. Contacts with the Mullen Creek layered mafic complex are typically sharp, but breccias and xenoliths of mafic units are locally observed. Previously mapped within the quadrangle as granite gneiss, pegmatized granite, and quartz-muscovite gneisses by Ruehr (1961), an older granite by Houston and others (1968), and a small felsic instrusive by Sutherland and Hausel (2004). Metamict zircons from sample HR-3F showed considerable uranium loss and resulted in reversely discordant $^{207}Pb/^{206}Pb$ ages between 1,710 and 1,600 Ma. Although no definitive date for this sample was acquired, the date range could be interpreted as an approximately 1,550 Ma (≤1,600 Ma) magmatic event where the zircons inherited older cores or as an older magmatic event (≥1,710 Ma) that recorded younger metamorphic alteration

Xbg **Biotite gneiss (Paleoproterozoic)**—Gray to tan to pink, fine- to medium-grained, mica-rich gneiss containing abundant biotite, quartz, plagioclase, and garnets, minor potassium feldspar and muscovite, and accessory sphene, apatite, and magnetite (Ruehr, 1961). This moderately foliated unit is exposed as elongated outcrops on Platte Ridge and grades from near-schistose to banded with quartz and garnet augens. Previously mapped by Ruehr (1961) as biotite granite gneiss and quartz-biotite gneiss and by Sutherland and Hausel (2004) as granite and quartz monzonite and related intrusive rocks 1,600–1,800 Ma

Xd **Diorite (Paleoproterozoic)**—Light-gray to gray, fine- to coarse-grained diorite composed of plagioclase, hornblende, and quartz. The diorite crops out in northeast–southwest-trending exposures in the center of the quadrangle and commonly contains dark-gray, very fine grained xenoliths of amphibolite. The term "xenolith" is used due to differences in average XRF major element composition and sharp, unzoned margin relationships between the diorite and amphibolite. The unit is locally crosscut by cm- to m-wide fine- to medium-grained granitic dikes. Contacts with the foliated granite (Xfg) are typically sheared. Previously mapped as granodiorite and quartz monzonite gneiss by Swetnam (1961). Although this unit displays brecciated and xenolithic textures similar to that of the Keystone Quartz Diorite transition zone observed on the Albany quadrangle by Sutherland and Kragh (2018), sample HR -4E yielded a younger date of 1,775±1.8 Ma, within error of the Lake Owen layered mafic complex (1,775.1±3.0 Ma; Sutherland and Kragh, 2018) and the Mullen Creek layered mafic complex (1,778±2 Ma; Loucks and others, 1988)

Mullen Creek layered mafic complex (Paleoproterozoic)—Layered mafic intrusion exposed in the northwest corner of the quadrangle. Previous regional mapping of the complex documented amphibolite, gabbro, olivine gabbro, anorthosite, diorite, metagabbro, metabasalt, metapyroxenite, and metadiabase units (Ruehr, 1961; Houston and others, 1968; McCallum and Orback, 1968; Ramirez, 1971; Donnelly, 1979, Edwards, 1983). Loucks and Glasscock (1989) indicate the Mullen Creek layered mafic complex is similar to the Lake Owen layered mafic complex (located on the Albany, Lake Owen, Foxpark, and Woods Landing quadrangles), but Houston and others (1968) note the Mullen Creek complex is larger and more deformed. Loucks and others (1988) reported a U-Pb age of 1,778±2 Ma from a Mullen Creek diorite, within error of a 1,775.1±3 Ma date from a Lake Owen pegmatitic gabbro-norite on the Albany quadrangle

Xmca **Mullen Creek amphibolite**—Gray to dark-gray to black, fine-grained, massive to weakly foliated amphibolite. Primarily composed of hornblende and plagioclase with minor biotite, magnetite, quartz, and pyroxene. Thin quartz and epidote veins crosscut the unit. The granitic felsic intrusive unit (Xgfi) interfingers with and crosscuts the Mullen Creek amphibolite, with local hybridization observed between the two units. The unit is bounded on the southwest by Mullen Creek gabbro and metagabbro, and on the east by the medium- to coarse-grained amphibolite and amphibolite gneiss unit (Xa). Discrete contacts are commonly obscured by soil cover but tend to be sharper with the small felsic intrusion and more gradational with the gabbro and amphibolite gneiss units

Xmcg **Mullen Creek gabbro and metagabbro**—Fine- to coarse-grained, dark-gray to dark-green, massive to weakly foliated gabbro. Major minerals include hornblende, pyroxene, and plagioclase, with localized unaltered outcrops containing olivine phases. Gradation into anorthosite and bluish-green, chlorite-rich, sometimes crenulated schist, was observed locally within the quadrangle. Weathers to rounded outcrops that are rust to brown in color. Isolated pods of metagabbro occur near contacts with the granitic felsic intrusive unit (Xgfi) and are indicated by large, sometimes elongated, pyroxene grains rimmed by fine-grained hornblende and plagioclase

Xk **Keystone Quartz Diorite (Paleoproterozoic)**—Light- to medium-gray, medium- to coarse-grained, equigranular to porphyritic quartz diorite. Major mineralogy consists of plagioclase, quartz, and hornblende with accessory biotite, chlorite, epidote, microcline, and sphene (Currey, 1965; Houston and others, 1968). The unit intrudes the amphibolite and amphibolite gneiss (Xa) in the northeast portion of the quadrangle, typically as rounded outcrops with weak to moderate foliation. Contacts between the quartz diorite and adjacent mafic rocks are commonly gradational, and may display hybridization with, or xenoliths of, the surrounding country rock. Near shear zones, the unit displays ductile and mylonitic textures, but some brittle, small-scale displacement of individual grains and narrow veins was observed. Two U-Pb zircon dates within error of each other have been reported for the Keystone Quartz Diorite—1,781±7 Ma (Premo and Van Schmus, 1989) and 1,784.7±1.9 Ma from the Woods Landing quadrangle to the east (Campbell and Shelton, in press)

Xsg **Gabbro and metagabbro (Paleoproterozoic)**—Gray to dark-gray to dark-greenish-gray, medium- to coarse-grained gabbro composed of hornblende, pyroxene (commonly rimmed by hornblende), and plagioclase, with minor olivine, quartz, magnetite, and serpentine. The unit intrudes into the amphibolite and amphibolite gneiss (Xa) east of Pelton Creek in the southeast corner of the quadrangle. The gabbro grades into metagabbro along the margins of the unit where a weak fabric develops in larger pyroxene grains. The gabbro and metagabbro commonly becomes schistose or amphibolitized near contacts with Xa. This unit is generally differentiated from the Mullen Creek gabbro and metagabbro by spatial location

Xa **Amphibolite and amphibolite gneiss (Paleoproterozoic)**—Undifferentiated gray to dark-gray amphibolite lithologies dominated by hornblende and plagioclase with minor chlorite, epidote, and pyroxene. This unit includes fine- to coarse-grained, massive to weakly foliated amphibolite, thinly to coarsely banded amphibolite gneiss (mm- to m-scale bands), and locally migmatitic amphibolite gneiss with disseminated feldspar leucosomes (mm- to cm-scale). Pegmatites are commonly found within or parallel to this unit. Undeformed amphibolite outcrops dominate the quadrangle north of Illinois Creek and Platte Ridge and east of Pelton Creek, but abruptly grade into amphibolite gneiss near shear zones and intrusive bodies such as the Mullen Creek layered mafic complex and the Keystone Quartz Diorite. South of Platte Ridge and west of Pelton Creek, this unit is exposed as narrow, resistant outcrops and dikes trending along foliation within the foliated granite (Xfg). These thin amphibolite outcrops are typically undeformed, but become gneissic within the hinges of regional folds and near some contacts with felsic units. Inter mingling with felsic units is common, creating wide transition zones between predominantly mafic and predominantly felsic rocks. The mylonitic amphibolite phase was observed along Douglas Creek and near the confluence of Pelton Creek with Illinois Creek. Previously mapped as hornblende gneiss, amphibole gneiss, or a layered mafic/felsic sequence (Myers, 1958; Ruehr, 1961; Swetnam, 1961; Houston and others, 1968; Sutherland and Hausel, 2004)

Xvf **Quartzofeldspathic gneiss (Paleoproterozoic)**—Predominantly gray to pink to orange, fine- to medium-grained gneiss composed of strongly foliated felsic bands of potassium feldspar, plagioclase, and quartz, with minor hornblende, biotite, and epidote. The felsic bands alternate with thinner bands of foliated mafic minerals, including hornblende, pyroxene, and biotite. Where the gneissic fabric is strongest, individual bands are only mm- to cm-thick. Outcrops are primarily located along shear zones and display ductile deformation textures such as potassium feldspar augens and local mylonitic fabrics. Contacts with the foliated granite (Xfg) are typically gradational, but contacts with amphibolite and amphibolite gneiss (Xa) vary from gradational and intermingled to sharp. Previously mapped by Myers (1958), Swetnam (1961), and Houston and others (1968) as a more extensive unit that spatially included this map's Xfg

Xfg **Foliated granite (Paleoproterozoic)**—Whitish-gray to tan to pink to orange, medium- to coarse-grained granite dominated by quartz, potassium feldspar, and biotite. Garnets and iron oxide minerals were observed locally. Foliation is weak throughout most of the unit, but becomes moderate near shear zones and contacts with intruding mafic units. Exposures of foliated granite dominate the quadrangle south of Platte Ridge and west of Pelton Creek and are typically bulbous or wedge-shaped with weathering patterns following foliation planes. The unit grades into the quartzofeldspathic gneiss (Xvf) along shear zones. At intersections of shear zones along Pelton Creek and within the hinge of a regional fold near the confluence of Elkhorn Creek and the North Platte River west of the Copper King mine, the foliated granite also grades into a biotite-muscovite-quartz schist. Includes units previously mapped as quartz monzonite gneiss and pegmatized quartz monzonite gneiss (Myers, 1958; Swetnam, 1961), quartzofeldspathic gneiss (Houston and others, 1968), and felsic gneiss (Sutherland and Hausel, 2004). Sample HR-2G near the Copper King mine yielded a reversely discordant U-Pb date of 1,562±3.8 Ma and significant uranium loss. If the uranium loss is recent, this date can be interpreted as magmatic, which overlaps with a 1,514±36 Ma date from a pegmatite dike in the Woods Landing quadrangle (Campbell and Shelton, in press) and also with regional 1.65–1.55 Ma reactivation of the Cheyenne Belt in the Sierra Madre and Medicine Bow Mountains (Strickland, 2004; Sigler, 2008; Cubrich, 2017). Sample HR-6GR, from the southwest corner of the quadrangle within a folded dike swarm, returned a concordant 1,785±1.9 Ma age. The more than 200 Ma age difference in the samples suggests discrete intrusive pulses or metamorphic histories across the unit. More analyses are required to better define the timing of such magmatic and metamorphic events and possible further subdivision of the unit

Xmmz **Mixed-metamorphic zone (Paleoproterozoic)**—Interlayered metaigneous and meta-sedimentary rocks located in the southwest corner of the quadrangle. The dominant lithology in this unit is mylonitized garnet amphibolite gneiss containing mm- to cm-diameter garnet porphyroblasts. Other rock types include white to gray garnet-bearing quartzite with possible minor talc, fine- to medium-grained amphibolite, and fine-grained quartz-garnet-biotite schist that grades into gneiss. Multiple quartz-potassium feldspar pegmatites intrude the sequence along foliation. A large brecciated pegmatite was observed near the southeast edge of the unit. The unit is surrounded by weakly foliated granite and is fault-bounded on its northeast and southwest margins

DISCLAIMERS

Users of this map are cautioned against using the data at scales different from those at which the map was compiled. Using these data at a larger scale will not provide greater accuracy and is a misuse of the data.

The Wyoming State Geological Survey (WSGS) and the State of Wyoming make no representation or warranty, expressed or implied, regarding the use, accuracy, or completeness of the data presented herein, or of a map printed from these data. The act of distribution shall not constitute such a warranty. The WSGS does not guarantee the digital data or any map printed from the data to be free of errors or inaccuracies.

The WSGS and the State of Wyoming disclaim any responsibility or liability for interpretations made from, or any decisions based on, the digital data or printed map. The WSGS and the State of Wyoming retain and do not waive sovereign immunity.

The use of or reference to trademarks, trade names, or other product or company names in this publication is for descriptive or informational purposes only, or is pursuant to licensing agreements between the WSGS or State of Wyoming and software or hardware developers/vendors, and does not imply endorsement of those products by the WSGS or the State of Wyoming.

NOTICE TO USERS OF INFORMATION FROM THE WYOMING STATE GEOLOGICAL SURVEY

The WSGS encourages the fair use of its material. We request that credit be expressly given to the "Wyoming State Geological Survey" when citing information from this publication. Please contact the WSGS at 307-766-2286, ext. 224, or by email at wsgs-info@wyo.gov if you have questions about citing materials, preparing acknowledgments, or extensive use of this material. We appreciate your cooperation.

Individuals with disabilities who require an alternative form of this publication should contact the WSGS. For the TTY relay operator, call 800-877-9975.

For more information about the WSGS or to order publications and maps, go to www.wsgs.wyo.gov, call 307-766-2286, ext. 224, or email wsgs-info@wyo.gov.

NOTICE FOR OPEN FILE REPORTS PUBLISHED BY THE WSGS

Open File Reports are preliminary and usually require additional fieldwork and/or compilation and analysis; they are meant to be a first release of information for public comment and review. The WSGS welcomes any comments, suggestions, and contributions from users of the information.

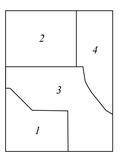

INDEX MAP SHOWING PREVIOUS MAPPING WITHIN THE HORATIO ROCK QUADRANGLE

1: Myers (1958); 2: Ruehr (1961); 3: Swetnam (1961); 4: Houston and others (1968)

REFERENCES

Campbell, E.A., and Shelton, C.R., in press, Preliminary geologic map of the Woods Landing quadrangle, Albany County, Wyoming: Wyoming State Geological Survey Open File Report 2018-3, scale 1:24,000.

Carnes, J.D., Chumley, A.S., and Samra, C.P., in press, Preliminary geologic map of the Foxpark quadrangle, Albany County, Wyoming: Wyoming State Geological Survey Open File Report 2018 -2, scale 1:24,000.

Chamberlain, K.R., 1998, Medicine Bow orogeny—Timing of deformation and model of crustal structure produced during continent-arc collision, ca. 1.78 Ga, southeastern Wyoming: Rocky Mountain Geology, v. 33, no. 2, p. 259–277.

Cubrich, B.T., 2017, Paleoproterozoic history of the Rocky Mountains —Using multiple geochronologic methods to unravel the Proterozoic structural history of polyphase deformation in highly deformed rocks: Laramie, University of Wyoming, M.S. thesis, 444 p., 5 pls.

Currey, D.R., 1965, The Keystone gold-copper prospect area, Albany County, Wyoming: Geological Survey of Wyoming [Wyoming State Geological Survey] Preliminary Report 3, 12 p., 1 pl.

Donnelly, M.E., 1979, Petrology and structure of a portion of the Precambrian Mu llen Creek metaigneous mafic complex, Medicine Bow Mountains, Wyoming: Fort Collins, Colorado State University, M.S. thesis, 162 p., 2 pls.

Dubendorfer, E.M., 1986, Structure, metamorphism, and kinematic history of the Cheyenne belt, Medicine Bow Mountains, southeastern Wyoming: Laramie, University of Wyoming, Ph.D dissertation, 323 p., 3 pls., scale 1:24,000 and 1:50,000.

Edwards, J.S., 1983, Petrology and contact relationships, SW portion Precambrian Mullen Creek mafic complex, Medicine Bow Mountains, Wyoming: Fort Collins, Colorado State University, M.S. thesis, 153 p., 2 pls., scale 1:10,226.

Frost, C.D., Frost, B.R., Chamberlain, K.R., and Edwards, B.R., 1999, Petrogenesis of the 1.43 Ga Sherman batholith, SE Wyoming, USA—A reduced, rapakivi-type anorogenic granite: Journal of Petrology, v. 40, no. 12, p. 1771–1,802.

Hills, F.A., Gast, P.W., Houston, R.S., and Swaibank, I.G., 1968, Precambrian geochronology of the Medicine Bow Mountains, southeastern Wyoming: Geological Society of America Bulletin, v. 79, p. 1,757–1,784.

Houston, R.S., McCallum, M.E., King, J.S., Ruehr, B.B., Myers, W.G. , Orback, C.J., King, J.R., Childers, M.O., Irwin Matus, Currey, D.R., Gries, J.C., Stensrud, H.L., Catanzaro, E.J., Swetnam, M.N., Michalek, D.D., and Blackstone, D.L., Jr., 1968, A regional study of rocks of Precambrian age in that part of the Medicine Bow Mountains lying in southeastern Wyoming—With a chapter on the relationship between Precambrian and Laramide structure: Geological Survey of Wyoming [Wyoming State Geological Survey] Memoir 1, 167 p., 35 pls. (Reprinted 1978.)

Jones, D.S., Snoke, A.W., Premo, W.R., and Chamberlain, K.R., 2010, New models for Paleoproterozoic orogenesis in the Cheyenne belt region—Evidence from the geology and U-Pb geochronology of the Big Creek Gneiss southeastern Wyoming: Geological Society of America Bulletin, v. 122, no. 11–12, p. 1,877–1,898.

Karlstrom, K.E., 1981, Late Archean and Early Proterozoic geologic history of metasedimentary rocks of the Medicine Bow Mountains, Wyoming: Laramie, University of Wyoming, Ph.D dissertation, 183 p., 3 pls.

Knight, S.H., 1990, Illustrated geologic history of the Medicine Bow Mountains and adjacent areas, Wyoming: Geological Survey of Wyoming [Wyoming State Geological Survey] Memoir 4, 48 p.

Loucks, R.R., and Glasscock, J.W., 1989, Petrology and PGE mineralization of the Early Proterozoic Lake Owen layered mafic intrusion, southern Wyoming, USA: Bulletin of the Geological Society of Finland, v. 61, p. 11–12.

Loucks, R.R., Premo, W.R., and Snyder, G.L., 1988, Petrology, structure, and age of the Mullen Creek layered mafic complex and age of arc accretion, Medicine Bow Mountains, Wyoming: Geological Society of America Abstracts with Programs, no. 20, p. A73.

McCallum, M.E., and Houston, R.S., 1985, Geologic map of the Albany quadrangle, Albany County, Wyoming (unpublished mineral files): Geological Survey of Wyoming [Wyoming State Geological Survey], 16 p., 1 pl., scale 1:24,000.

McCallum, M.E., and Orback, C.J., 1968, The New Rambler copper-gold-platinum district, Albany and Carbon counties, Wyoming: Geological Survey of Wyoming [Wyoming State Geological Survey] Preliminary Report 8, 12 p., 1 pl.

Myers, W.G., 1958, Geology of the Sixmile Gap area, Albany and Carbon counties, Wyoming: Laramie, University of Wyoming, M.S. thesis, 74 p., 3 pls.

Premo, W.R., and Loucks, R.R., 2000, Age and Pb-Sr-Nd isotopic systematics of plutonic rocks from the Green Mountain magmatic arc, southeastern Wyoming—Isotopic characterization of a Paleoproterozoic island arc system: Rocky Mountain Geology, v. 35, no. 1, p. 51–70.

Premo, W.R., and Van Schmus, W.R., 1989, Zircon geochronology of Precambrian rocks in southeastern Wyoming and northern Colorado, *in* Grambling, J.A. and Tewksbury, B.J., eds., Proterozoic geology of the southern Rocky Mountains: Geological Society of America Special Paper 235, p. 13–32.

Ramirez, Octavio, 1971, Petrology and structure of the Precambrian metaigneous sequence in the Savage Run Creek area, Carbon County, Wyoming: Fort Collins, Colorado State University, M.S. thesis, 117 p., 1 pl., scale 1:16,000.

Ruehr, B.B., 1961, Geology of Devils Gate area, Albany and Carbon counties, Wyoming: Laramie, University of Wyoming, M.S. thesis, 48 p., 1 pl., scale 1:24,000.

Sigler, J.T., 2008, The metamorphic and structural evolution of the Davis Peak area, northern Park Range, Colorado: Laramie, University of Wyoming, M.S. thesis, 259 p., 1 pl., scale 1:24,000.

Strickland, D.S., 2004, Structural and geochronologic evidence for the ca. 1.6 Ga reactivation of the Cheyenne belt, southeastern Wyoming: Laramie, University of Wyoming, M.S. thesis, 157 p.

Sutherland, W.M., and Hausel, W.D., 2004, Preliminary geologic map of the Saratoga 30′ x 60′ quadrangle, Carbon and Albany counties, Wyoming: Wyoming State Geological Survey Open File Report 04 -10, 34 p., 1 pl., scale 1:100,000.

Sutherland, W.M., and Hausel, W.D., 2005, Preliminary geologic map of the Keystone quadrangle, Albany and Carbon counties, Wyoming: Wyoming State Geological Survey Open File Report 05 -6, 21 p., 1 pl., scale 1:24,000.

Sutherland, W.M., and Kragh, N.A., 2018, Preliminary geologic map of the Albany quadrangle, Albany County, Wyoming: Wyoming State Geological Survey Open File Report 2018-1, 45 p., 1 pl., scale 1:24,000.

Sutherland, W.M., Stafford, J.E., Carroll, C.J., Gregory, R.W., and Kehoe, K.S., 2018, Mines and minerals map of Wyoming: Wyoming State Geological Survey, accessed September 2018, at http://wsgs.maps.arcgis.com/apps/webappviewer/index.html?id=af948a51f4954a81adeae8935440cd28.

Swetnam, M.N., 1961, Geology of the Pelton Creek area, Albany and Carbon counties, Wyoming: Laramie, University of Wyoming, M.S. thesis, 78 p., 13 pls., scale 1:15,500.

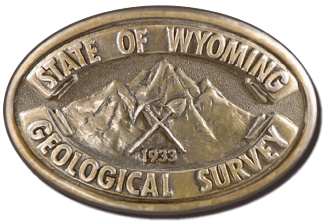

Interpreting the past, providing for the future

Preliminary Geologic Map of the Horatio Rock 7.5' Quadrangle, Carbon and Albany Counties, Wyoming

By Rachel N. Toner, Charles P. Samra, Adam S. Chumley, Kelsey S. Kehoe, and Andrea M. Loveland

Open File Report 2019-5
June 2019

Wyoming State Geological Survey

Erin A. Campbell, Director and State Geologist

Preliminary Geologic Map of the Horatio Rock 7.5' Quadrangle, Carbon and Albany Counties, Wyoming

By Rachel N. Toner, Charles P. Samra, Adam S. Chumley, Kelsey S. Kehoe, and Andrea M. Loveland

Layout by Christina D. George

Open File Report 2019-5
Wyoming State Geological Survey
Laramie, Wyoming: 2019

This Wyoming State Geological Survey (WSGS) Open File Report is preliminary and may require additional compilation and analysis. Additional data and review may be provided in subsequent years. For more information about the WSGS, or to download a copy of this Open File Report, visit www.wsgs.wyo.gov. The WSGS welcomes any comments and suggestions on this research. Please contact the WSGS at 307-766-2286, or email wsgs-info@wyo.gov.

Citation: Toner, R.N., Samra, C.P., Chumley, A.S., Kehoe, K.S., and Loveland, A.M., 2019, Preliminary geologic map of the Horatio Rock 7.5' quadrangle, Carbon and Albany counties, Wyoming: Wyoming State Geological Survey Open File Report 2019-5, 21 p., scale 1:24,000.

Table of Contents

List of Figures

List of Tables

INTRODUCTION

The Horatio Rock 7.5' quadrangle is located in the southern Medicine Bow Mountain Range in southeastern Wyoming and straddles Carbon and Albany counties (fig. 1). Bedrock mapping of the Horatio Rock quadrangle is part of a larger, multi-year effort to investigate the relationships between the structural and petrologic history that influenced mineralization of Au, Ag, Cu, platinum-group elements (PGEs), V, Ti, Fe, and rare earth elements (REEs) within the Southern Medicine Bow Mountains Mining District. This quadrangle lies south of the Cheyenne belt, and exposes Proterozoic-age island-arcs, metavolcanics, and intrusive granitic and mafic rocks. The Copper Ridge historic mining district spans the southern portion of the quadrangle and extends into the Foxpark quadrangle to the east (Swetnam, 1961; Hausel, 1997). Within the Horatio Rock quadrangle, the Copper Ridge historic mining district includes numerous small prospect pits, one patented lode claim known as the Copper King mine or shaft (Swetnam, 1961; Hausel, 1997; Sutherland and others, 2018), and numerous historic and active placer claims along Pelton and Douglas creeks.

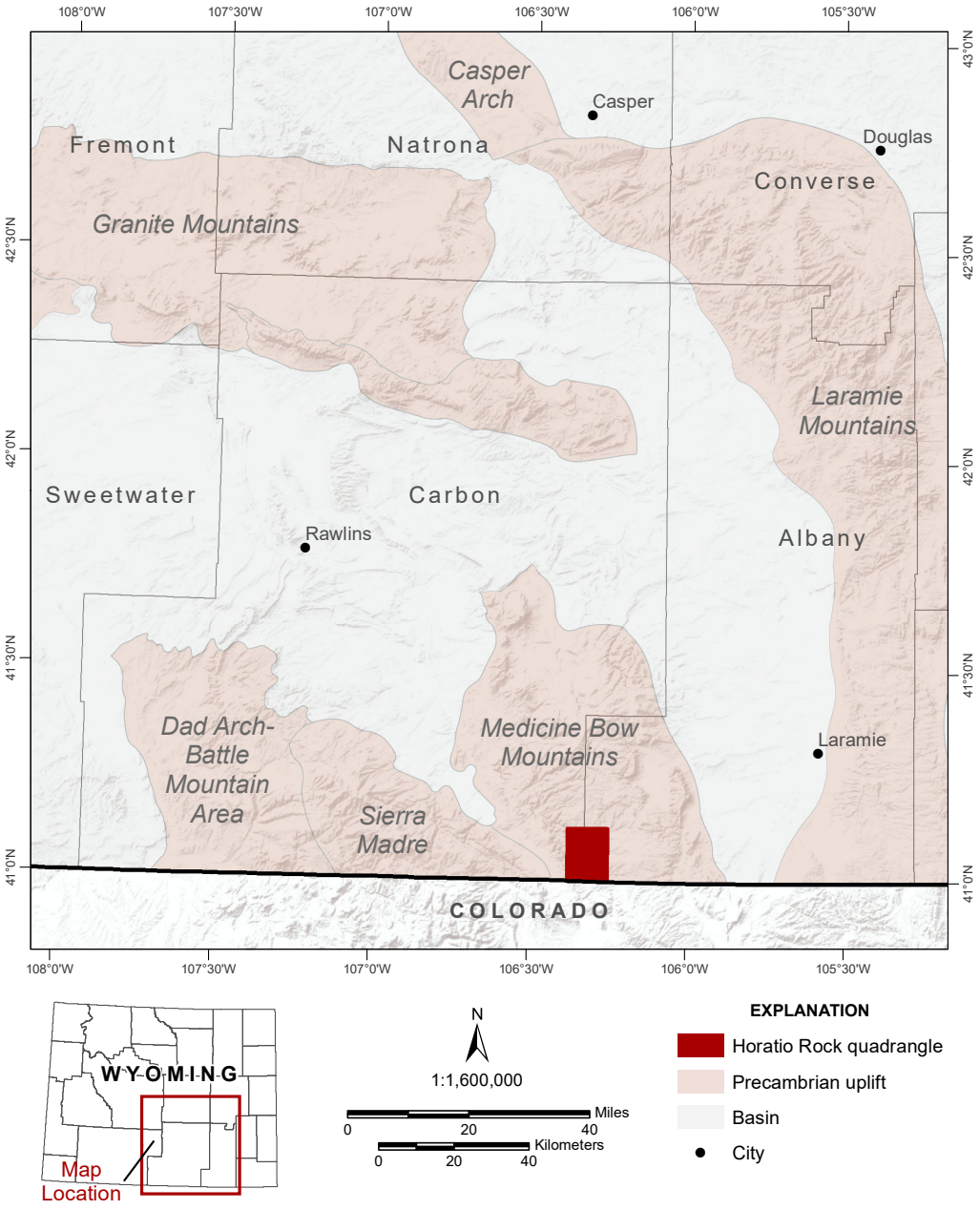

Figure 1. Location of Horatio Rock quadrangle (red rectangle).

Previous field mapping efforts within the Horatio Rock quadrangle were conducted by Myers (1958), Swetnam (1961), and Ruehr (1961), while Houston and others (1968) and Sutherland and Hausel (2004) compiled regional maps that included this map area. These previous geologic interpretations were referenced and used for remote areas where current access and travel was restricted. Bedrock mapping at the 1:24,000 scale has been completed for the surrounding Keystone (Sutherland and Hausel, 2005), Albany (Sutherland and Kragh, 2018), Foxpark (Carnes and others, in press), and Woods Landing (Campbell and Shelton, in press) quadrangles.

Rock unit identification and description, foliation measurement, structural feature identification, and sample collection was conducted on the Horatio Rock quadrangle from June through early October 2018. Field mapping efforts were supported by satellite imagery interpretation in areas with minimal vegetation cover.

The map was completed in cooperation with the U.S. Geological Survey 2018 StateMap grant award #G18AC00150 to the Wyoming State Geological Survey.

SAMPLES

More than 100 grab samples were collected from the Horatio Rock quadrangle, primarily from outcrops or where source was implied by abundant float of one lithology. A total of 46 samples were submitted for geochemical, petrographic, and geochronological analyses. Grab sample analysis may yield elemental concentrations and petrographic features representative of that particular sample and not the rock unit as a whole.

THIN SECTIONS

A total of 40 thin sections were prepared by Wagner Petrographics of Lindon, Utah, (4 polished and 36 unpolished). Mineralogy, textures, and microstructures observed from the thin sections were used to augment rock unit descriptions, where applicable.

GEOCHEMICAL ANALYSES

ALS Chemex of Reno, Nevada, analyzed 28 Horatio Rock samples for whole rock chemistry, including trace elements and REEs. Of the 28 samples, 6 were also analyzed for either PGEs, gold, or both. Samples submitted for geochemical analysis were selected to assist in lithology identification, establish relationships between the different lithologies, and evaluate the composition and mineralization potential of rocks within the quadrangle.

Analyses were conducted using inductively coupled plasma (ICP) atomic emission spectrometry, ICP mass spectrometry, combustion furnace, fire assay, and atomic absorption spectroscopy. Tables 1 and 2 provide results of geochemical analyses, sample locations, and sample units. The majority of the returned results indicated negligible to undetectable concentrations of base and precious metals as well as REEs concentration.

Table 1. Whole rock analyses for samples collected within the Horatio Rock quadrangle. Map unit abbreviations include: Xa—amphibolite and amphibolite gneiss; Xfg—foliated granite; Xgfi—granitic felsic intrusive; Xmca—Mullen Creek amphibolite; Xmcg—Mullen Creek gabbro and metagabbro; Xvf—quartzofeldspathic gneiss; Xd—diorite; Xsg—gabbro and metagabbro. Abbreviated analytical methods are defined as follows: ME-ICP06—analysis by inductively coupled plasma (ICP) atomic emission spectrometry; C-IR07—total carbon by combustion furnace; and S-IR08—total sulfur by combustion furnace. Significant digits as reported from ALS Chemex lab.

SAMPLE	Map Unit	Latitude (WGS84)	Longitude (WGS84)	SiO_2 %	Al_2O_3 %	Fe_2O_3 %	CaO %	MgO %	Na_2O %	K_2O %	Cr_2O_3 %	TiO_2 %	MnO %	P_2O_5 %	SrO %	BaO %	LOI %	Total %	C %	S %
HR-2G	Xfg	41.01530	-106.26666	76	12.3	1.71	0.72	0.1	2.9	5.37	<0.002	0.09	0.04	0.01	<0.01	0.01	0.38	99.63	0.01	<0.01
HR-3F	Xgfi	41.11563	-106.32079	76.4	13.8	0.73	0.91	0.21	4.45	3.69	<0.002	0.04	0.03	0.04	<0.01	<0.01	0.51	100.81	0.04	<0.01
HR-4E	Xd	41.06760	-106.31586	51.3	18.5	9.06	8.49	3.97	3.87	0.88	0.007	0.64	0.18	0.24	0.08	0.04	1.35	98.61	0.01	<0.01
HR-6GR	Xfg	41.00938	-106.35213	76.6	12.65	2.29	0.74	0.09	3.53	4.67	<0.002	0.16	0.01	0.03	0.01	0.17	0.28	101.23	0.02	<0.01
18HRAC-02	Xsg	41.10933	-106.26721	45.6	10.45	9.73	11.75	18.85	0.81	0.11	0.195	0.25	0.16	0.05	0.03	0.01	1.95	99.95	0.11	0.03
18HRAC-08	Xmcg	41.11322	-106.33051	45.9	7.43	10.1	6.71	21.5	0.32	0.07	0.424	0.23	0.18	0.08	<0.01	<0.01	5.11	98.05	0.03	0.01
18HRAC-10	Xfg	41.05021	-106.26652	77.4	12.2	1.92	0.8	0.44	4	3.61	0.003	0.11	0.01	0.02	0.01	0.17	0.42	101.11	0.02	<0.01
18HRAC-15	quartz vein in Xfg	41.02126	-106.26392	96.4	0.3	2.51	0.12	0.33	0.02	0.04	0.008	0.01	<0.01	<0.01	<0.01	0.01	1.17	100.92	0.07	0.45
18HRAC-16	quartz vein in Xfg	41.02178	-106.26476	91.4	2.24	2.84	0.05	0.21	0.01	0.73	0.003	0.03	<0.01	0.01	<0.01	0.01	1.99	99.52	0.2	0.02
18HRAC-18	small felsic finger in Xa	41.08188	-106.26293	73.7	14.35	1.7	1.55	0.26	3.39	4.66	<0.002	0.12	0.02	0.05	0.02	0.1	0.49	100.41	0.02	<0.01
18HRAC-19	Xsg	41.03474	-106.26633	44.8	16.45	17	10.75	5.52	1.78	0.48	<0.002	1.32	0.19	0.17	0.05	0.02	0.51	99.04	0.02	0.01
18HRCS-02	Xa	41.12052	-106.29495	48.2	20.7	6.78	14.35	7.03	1.41	0.21	0.054	0.28	0.11	0.02	0.07	0.01	0.8	100.02	0.05	0.01
18HRCS-08	quartz vein in Xmca	41.11332	-106.33057	97.3	1.57	1.04	0.46	0.64	0.29	0.03	0.006	0.04	0.01	0.01	<0.01	<0.01	0.46	101.86	0.02	<0.01
18HRCS-14	quartz vein in Xvf	41.04827	-106.27354	73	12.1	4.55	2.76	2.4	3.94	0.32	0.011	0.43	0.06	0.1	0.03	0.01	1.71	101.42	0.02	0.01
18HRCS-18	Xfg	41.00073	-106.30683	75.8	12.8	2.38	0.78	0.13	3.52	4.85	<0.002	0.15	0.02	0.02	0.01	0.21	0.27	100.94	0.02	<0.01
18HRCS-22	Xfg	41.00151	-106.35375	76	12.7	3.08	0.69	0.21	3.15	5.13	<0.002	0.27	0.02	0.01	0.01	0.26	0.4	101.93	0.02	<0.01
18HRCS-24	Xg	41.08636	-106.34892	74.5	13.95	2.22	1.64	0.42	3.36	4.12	<0.002	0.21	0.04	0.07	0.03	0.13	0.46	101.15	0.04	<0.01
18HRCS-29	Xd (fine-grained)	41.06416	-106.33299	47.7	16.2	9.59	11.4	9.2	1.72	0.64	0.051	0.4	0.16	0.09	0.03	0.05	1.93	99.16	0.04	0.02
18HRCS-30	Xd	41.06406	-106.31483	47.9	14.75	15.35	9.57	5.47	2.86	1.03	0.002	1.06	0.17	0.12	0.05	0.07	0.96	99.36	0.03	0.02
18HRCS-32	Xfg	41.01982	-106.30233	50.1	12.4	15.3	15.85	3.17	0.12	0.14	<0.002	0.43	0.34	0.16	0.05	<0.01	1.49	99.55	0.03	<0.01
18HRCS-35	Xfg	41.05346	-106.33513	76.9	13.15	2.13	1.81	0.18	5.65	0.55	<0.002	0.22	0.02	0.02	0.02	0.03	0.48	101.16	0.05	0.01
18HRRT-03	Xsg	41.10704	-106.27575	44.8	16.25	14.75	12.05	7.21	1.36	0.62	0.006	0.86	0.17	0.06	0.05	0.04	1	99.23	0.04	0.02
18HRRT-05	Xmca	41.11622	-106.32195	42.8	10.2	10.45	7.21	21.9	0.3	0.05	0.179	0.32	0.21	0.13	<0.01	<0.01	6.08	99.83	0.03	0.01
18HRRT-11	Xa	41.08903	-106.31134	45.3	19.35	5.83	13.75	9.33	0.57	1.81	0.073	0.14	0.1	0.01	0.1	0.02	3.25	99.63	0.06	0.01
18HRKK-04	Xmcg	41.10524	-106.31865	45.8	14.8	10.5	8.67	17.5	1.28	0.09	0.054	0.15	0.15	0.02	0.06	0.01	0.59	99.67	0.11	0.03
18HRKK-07	Xfg	41.05084	-106.31445	76.6	12.9	2.6	1.4	0.23	4.13	2.91	<0.002	0.16	0.05	0.02	0.02	0.23	0.32	101.57	0.03	0.01
HR-1A	Xa	41.01204	-106.35991	47.6	15.5	10.9	11	8.47	2.42	0.66	0.045	0.86	0.18	0.14	0.03	0.02	1.23	99.06	0.03	<0.01
HR-5C	Xa	41.00935	-106.35191	72.9	13.95	2.99	2.28	0.99	5.03	1.32	<0.002	0.35	0.04	0.11	0.04	0.05	0.43	100.48	0.02	<0.01
Analytical Method:				ME-ICP06													OA-GRA05	TOT-ICP06	C-IR07	S-IR08

Table 2. Trace element analyses for samples collected within the Horatio Rock quadrangle. Map unit abbreviations include: Xa—amphibolite and amphibolite gneiss; Xfg—foliated granite; Xgfi—granitic felsic intrusive; Xmca—Mullen Creek amphibolite; Xmcg—Mullen Creek gabbro and metagabbro; Xvf—quartzofeldspathic gneiss; Xd—diorite; Xsg—gabbro and metagabbro. Abbreviated analytical methods are defined as: ME-MS81—analysis by ICP mass spectrometry (MS); ME-MS42—analysis by ICP-MS; ME-4ACD81—analysis by ICP atomic emissions spectrometry (AES); Cu-OG62—analysis by ICP or atomic absorption spectroscopy (AAS); Au-AA25—analysis by fire assay and AAS; and PGM-ICP24—analysis by fire assay and ICP-AES. Significant digits as reported from ALS Chemex lab.

SAMPLE	Map Unit	Latitude (WGS84)	Longitude (WGS84)	Ag ppm	As ppm	Au ppm	Au ppm	Ba ppm
HR-2G	Xfg	41.01530	-106.26666	<0.5	2			54.8
HR-3F	Xgfi	41.11563	-106.32079	<0.5	0.8			27.4
HR-4E	Xd	41.06760	-106.31586	<0.5	2.3			370
HR-6GR	Xfg	41.00938	-106.35213	<0.5	0.7			1,435
18HRAC-02	Xsg	41.10933	-106.26721	<0.5	1			64
18HRAC-08	Xmcg	41.11322	-106.33051	<0.5	3	0.02	<0.001	41.2
18HRAC-10	Xfg	41.05021	-106.26652	<0.5	1.7			1575
18HRAC-15	quartz vein in Xfg	41.02126	-106.26392	0.7	13.3	0.01	<0.001	71.4
18HRAC-16	quartz vein in Xfg	41.02178	-106.26476	1.1	23.7	<0.01	0.001	104
18HRAC-18	small felsic finger in Xa	41.08188	-106.26293	<0.5	2.2			884
18HRAC-19	Xsg	41.03474	-106.26633	<0.5	2.7			214
18HRCS-02	Xa	41.12052	-106.29495	<0.5	1.6			102.5
18HRCS-08	quartz vein Xmca	41.11332	-106.33057	<0.5	0.4			22.3
18HRCS-14	quartz vein in Xvf	41.04827	-106.27354	<0.5	0.6	<0.01		97.8
18HRCS-18	Xfg	41.00073	-106.30683	<0.5	1.3			1,970
18HRCS-22	Xfg	41.00151	-106.35375	<0.5	1.3			2,430
18HRCS-24	Xg	41.08636	-106.34892	<0.5	1.4			1,210
18HRCS-29	Xd (fine-grained)	41.06416	-106.33299	0.5	5.7			425
18HRCS-30	Xd	41.06406	-106.31483	0.6	2.4			659
18HRCS-32	Xfg	41.01982	-106.30233	<0.5	1.5	<0.01	<0.001	25.4
18HRCS-35	Xfg	41.05346	-106.33513	0.5	1.3			317
18HRRT-03	Xsg	41.10704	-106.27575	0.6	8.2			333
18HRRT-05	Xmca	41.11622	-106.32195	<0.5	1.2		<0.001	29
18HRRT-11	Xa	41.08903	-106.31134	<0.5	2.2			197
18HRKK-04	Xmcg	41.10524	-106.31865	0.8	4.3			138.5
18HRKK-07	Xfg	41.05084	-106.31445	<0.5	1.7			2,130
HR-1A	Xa	41.01204	-106.35991	<0.5	0.5			163.5
HR-5C	Xa	41.00935	-106.35191	<0.5	0.6			418
Analytical Method:				ME-4ACD81	ME-MS42	Au-AA25	PGM-ICP24	ME-MS81

Table 2 continued.

SAMPLE	Bi ppm	Cd ppm	Ce ppm	Co ppm	Cr ppm	Cs ppm	Cu %	Cu ppm	Dy ppm
HR-2G	0.03	<0.5	85	2	10	2.17		8	4.42
HR-3F	0.07	<0.5	10.3	1	10	2.95		5	5.34
HR-4E	0.02	<0.5	36.2	25	60	0.47		61	3.38
HR-6GR	<0.01	<0.5	110.5	1	10	0.47		2	8.66
18HRAC-02	0.01	<0.5	5.6	71	1,420	0.09		67	1.09
18HRAC-08	0.03	<0.5	22.2	80	3,220	0.08		52	1.13
18HRAC-10	0.04	<0.5	84	1	30	0.26		14	5.83
18HRAC-15	1.46	<0.5	1.5	9	60	0.03	1.6	>10,000	0.78
18HRAC-16	1.6	<0.5	8.9	13	30	0.65	2.18	>10,000	2.08
18HRAC-18	0.02	<0.5	25	3	10	7.09		5	4.57
18HRAC-19	0.01	0.9	17.2	45	10	0.74		58	2.97
18HRCS-02	0.01	<0.5	8	34	400	0.22		6	1.33
18HRCS-08	0.03	<0.5	3.1	3	50	0.05		2	0.16
18HRCS-14	0.04	<0.5	28.4	14	90	0.13		415	1.72
18HRCS-18	0.01	<0.5	68.8	2	10	0.76		5	6.05
18HRCS-22	0.01	<0.5	114	2	10	0.41		4	9.16
18HRCS-24	0.2	<0.5	51.4	2	10	2.87		4	1.84
18HRCS-29	0.07	0.5	12.6	52	390	0.58		93	2.26
18HRCS-30	0.05	0.5	26.6	48	20	0.23		15	2.85
18HRCS-32	0.16	0.6	105	26	10	0.07		95	7.38
18HRCS-35	0.12	<0.5	136.5	3	10	0.13		3	4.94
18HRRT-03	0.02	0.6	23.4	53	50	0.43		292	2.55
18HRRT-05	0.03	0.5	9.9	89	1280	0.07		29	1.42
18HRRT-11	0.03	<0.5	3.6	38	550	1.94		21	0.69
18HRKK-04	0.02	0.5	4.6	72	400	0.09		40	0.51
18HRKK-07	0.01	<0.5	76.6	1	20	0.14		8	6.14
HR-1A	0.03	0.7	13.1	49	340	0.27		72	3.69
HR-5C	0.01	<0.5	108	6	20	0.69		13	5.21
Analytical Method:	ME-MS42	ME-4ACD81	ME-MS81	ME-4ACD81	ME-MS81	ME-MS81	Cu-OG62	ME-4ACD81	ME-MS81

Table 2 continued.

SAMPLE	Er ppm	Eu ppm	Ga ppm	Gd ppm	Ge ppm	Hf ppm	Hg ppm	Ho ppm	In ppm
HR-2G	2.64	0.24	16.6	3.74	<5	4	<0.005	0.9	0.017
HR-3F	3.57	0.09	24.3	4	<5	2.4	<0.005	1.12	<0.005
HR-4E	2.04	1.34	24.6	4.02	<5	1.1	<0.005	0.78	0.016
HR-6GR	5.82	1.28	23.6	6.92	<5	9.9	<0.005	1.79	0.043
18HRAC-02	0.62	0.38	8.2	1.2	<5	0.4	<0.005	0.24	0.006
18HRAC-08	0.82	0.37	7.9	1.52	<5	1.3	<0.005	0.24	<0.005
18HRAC-10	3.31	0.55	20.6	4.09	<5	6.4	<0.005	1.15	0.061
18HRAC-15	0.52	0.07	0.7	0.49	<5	<0.2	0.007	0.13	0.2
18HRAC-16	1.38	0.15	6.2	1.68	<5	0.6	0.015	0.47	0.044
18HRAC-18	3.33	0.78	19.3	3.36	<5	4.5	<0.005	1	0.007
18HRAC-19	1.58	0.85	21.5	2.82	<5	0.9	0.005	0.57	0.013
18HRCS-02	0.79	0.46	16.8	1.33	<5	0.5	0.006	0.26	<0.005
18HRCS-08	0.15	0.11	1.8	0.18	<5	<0.2	<0.005	0.04	<0.005
18HRCS-14	1.08	0.7	14.9	2.32	<5	2	<0.005	0.38	0.018
18HRCS-18	3.81	1.53	23	6.36	<5	11.9	<0.005	1.28	0.039
18HRCS-22	5.63	2.3	18.1	10.7	<5	11.2	0.007	1.96	0.082
18HRCS-24	1.18	0.61	16.7	2.18	<5	4.9	<0.005	0.44	0.006
18HRCS-29	1.6	0.61	14	1.89	<5	0.9	0.056	0.52	0.007
18HRCS-30	1.76	0.93	20.8	3.05	<5	1.5	0.019	0.54	0.02
18HRCS-32	4.98	2.93	27.2	7.22	<5	4.4	<0.005	1.69	0.088
18HRCS-35	3.62	0.64	20.4	3.6	<5	10.5	0.007	1.04	0.033
18HRRT-03	1.76	0.62	20.1	2.73	<5	0.9	0.016	0.52	0.012
18HRRT-05	0.79	0.59	9.6	1.32	<5	0.7	<0.005	0.26	0.007
18HRRT-11	0.39	0.28	11.8	0.6	<5	0.3	<0.005	0.12	<0.005
18HRKK-04	0.36	0.28	10.7	0.41	<5	0.3	0.031	0.1	<0.005
18HRKK-07	3.64	2.18	21	5.42	<5	8.4	0.011	1.27	0.082
HR-1A	2.53	0.89	18.9	3.32	<5	1.3	<0.005	0.73	0.009
HR-5C	2.89	1.07	24.5	6.33	<5	8	<0.005	0.96	0.045
Analytical Method:	ME-MS81	ME-MS81	ME-MS81	ME-MS81	ME-MS81	ME-MS81	ME-MS42	ME-MS81	ME-MS42

Table 2 continued.

SAMPLE	La ppm	Li ppm	Lu ppm	Mo ppm	Nb ppm	Nd ppm	Ni ppm	Pb ppm	Pd ppm
HR-2G	32.3	20	0.36	<1	12.7	25.4	3	18	
HR-3F	5.4	<10	0.62	<1	38.3	6.6	3	41	
HR-4E	16.1	10	0.28	<1	3	19.7	20	2	
HR-6GR	38.3	<10	0.83	1	13.7	37.4	1	10	
18HRAC-02	2.7	<10	0.08	<1	0.8	3.7	421	<2	
18HRAC-08	10.1	10	0.15	<1	2.8	10.8	1,110	<2	0.002
18HRAC-10	19.7	<10	0.59	<1	16.6	21.8	11	6	
18HRAC-15	1.1	<10	0.06	20	0.2	1.8	22	7	0.002
18HRAC-16	4.1	<10	0.17	26	2.5	6.2	8	7	0.003
18HRAC-18	12.1	10	0.54	<1	20.1	12.7	2	29	
18HRAC-19	7.6	<10	0.21	1	3.1	11.3	4	<2	
18HRCS-02	3.7	<10	0.09	1	1.2	4.8	83	<2	
18HRCS-08	1.6	<10	0.02	2	0.5	1.4	12	4	
18HRCS-14	14.2	10	0.2	2	7.9	13.5	28	5	
18HRCS-18	42.4	<10	0.62	1	12.3	40.6	3	13	
18HRCS-22	54.9	<10	0.8	<1	10.8	57.9	2	21	
18HRCS-24	21.8	20	0.25	1	10.2	14.8	3	17	
18HRCS-29	7.3	30	0.25	1	2.1	8.1	207	5	
18HRCS-30	12.5	10	0.21	1	3.2	15	56	3	
18HRCS-32	56.6	10	0.76	2	9.5	45.2	17	8	0.001
18HRCS-35	39.3	<10	0.63	<1	15.4	26	3	5	
18HRRT-03	10.4	10	0.26	1	3.6	13.2	47	<2	
18HRRT-05	5.8	20	0.13	<1	1.7	7.4	845	<2	0.006
18HRRT-11	1.5	30	0.06	<1	0.7	2.2	113	<2	
18HRKK-04	2	<10	0.04	1	0.4	2.7	537	<2	
18HRKK-07	28.6	<10	0.59	1	15.6	30.2	8	6	
HR-1A	5.4	20	0.3	<1	1.6	9.6	166	3	
HR-5C	38.8	10	0.35	1	11.4	43.2	5	5	
Analytical Method:	ME-MS81	ME-4ACD81	ME-MS81	ME-4ACD81	ME-MS81	ME-MS81	ME-4ACD81	ME-4ACD81	PGM-ICP24

Table 2 continued.

SAMPLE	Pr ppm	Pt ppm	Rb ppm	Re ppm	Sb ppm	Sc ppm	Se ppm	Sm ppm	Sn ppm
HR-2G	8.03		144	<0.001	0.05	1	<0.2	4.85	1
HR-3F	1.52		179	<0.001	0.07	4	<0.2	2.57	3
HR-4E	4.66		26.4	<0.001	0.09	20	<0.2	3.91	1
HR-6GR	10.15		91.2	<0.001	<0.05	2	<0.2	7.54	2
18HRAC-02	0.87		2.1	<0.001	0.05	40	0.2	1.07	<1
18HRAC-08	2.74	0.007	1.4	<0.001	0.11	19	<0.2	1.63	<1
18HRAC-10	5.87		59	<0.001	0.07	2	0.2	5.25	2
18HRAC-15	0.34	<0.005	1.6	0.006	0.16	<1	10.5	0.48	<1
18HRAC-16	1.35	<0.005	41.6	0.01	0.05	1	12.4	1.68	<1
18HRAC-18	3.18		94.4	<0.001	0.15	3	0.2	3.14	1
18HRAC-19	2.52		10.2	<0.001	0.21	42	0.2	2.53	1
18HRCS-02	1.1		2.9	<0.001	0.17	23	0.2	0.86	<1
18HRCS-08	0.39		1.2	<0.001	0.09	3	<0.2	0.26	<1
18HRCS-14	3.56		7.4	<0.001	<0.05	12	0.2	2.71	4
18HRCS-18	10.6		82	<0.001	0.09	1	<0.2	7.79	2
18HRCS-22	14.25		68.8	<0.001	0.09	7	<0.2	11.1	3
18HRCS-24	4.49		131	<0.001	0.18	3	<0.2	2.52	1
18HRCS-29	1.91		17.5	<0.001	0.69	36	0.2	1.94	<1
18HRCS-30	3.38		17.5	<0.001	0.48	40	<0.2	3.54	1
18HRCS-32	12.05	<0.005	3.3	<0.001	0.08	17	<0.2	8.09	4
18HRCS-35	8.24		3.8	<0.001	0.36	6	<0.2	4.78	2
18HRRT-03	3.17		8.8	<0.001	0.27	49	0.6	2.89	1
18HRRT-05	1.79	0.009	0.9	<0.001	0.05	16	<0.2	1.6	<1
18HRRT-11	0.54		110.5	<0.001	0.42	29	0.2	0.66	<1
18HRKK-04	0.58		1.7	<0.001	0.55	13	0.2	0.53	<1
18HRKK-07	7.58		36.8	<0.001	0.21	3	<0.2	6.5	2
HR-1A	1.94		22.8	<0.001	0.16	38	0.4	2.37	<1
HR-5C	11.4		51.7	0.001	<0.05	5	0.3	7.82	2
Analytical Method:	ME-MS81	PGM-ICP24	ME-MS81	ME-MS42	ME-MS42	ME-4ACD81	ME-MS42	ME-MS81	ME-MS81

Table 2 continued.

SAMPLE	Sr ppm	Ta ppm	Tb ppm	Te ppm	Th ppm	Tl ppm	Tm ppm	U ppm	V ppm
HR-2G	22.6	0.8	0.72	<0.01	19.6	0.33	0.35	2.4	6
HR-3F	23.9	4.9	0.8	<0.01	13.4	0.06	0.56	3.03	7
HR-4E	720	0.3	0.54	0.01	1.79	0.04	0.25	0.76	210
HR-6GR	82.6	0.8	1.33	<0.01	11.2	0.08	0.83	2.54	7
18HRAC-02	255	0.2	0.18	0.01	0.23	<0.02	0.09	0.28	115
18HRAC-08	37.8	0.3	0.21	0.04	1.23	<0.02	0.11	0.39	105
18HRAC-10	96.9	1.1	0.74	<0.01	7.66	<0.02	0.51	3.02	16
18HRAC-15	4.7	0.2	0.14	0.28	0.15	0.05	0.06	16.95	21
18HRAC-16	6.8	0.3	0.34	0.71	1.17	0.04	0.18	16.4	63
18HRAC-18	199	2.2	0.58	<0.01	3.12	0.16	0.41	1.94	12
18HRAC-19	495	0.3	0.42	0.02	0.53	0.04	0.19	0.34	605
18HRCS-02	619	0.2	0.2	0.01	0.26	<0.02	0.11	0.22	114
18HRCS-08	38.3	0.2	0.03	<0.01	0.11	<0.02	0.02	0.16	18
18HRCS-14	286	0.5	0.28	<0.01	2.71	<0.02	0.15	1.2	68
18HRCS-18	83.9	0.6	0.99	<0.01	7.43	0.03	0.57	3.04	10
18HRCS-22	94.4	0.4	1.49	<0.01	10.1	0.11	0.75	3.2	9
18HRCS-24	238	1	0.37	0.05	10.85	0.4	0.19	2.7	18
18HRCS-29	270	0.3	0.34	0.04	0.58	0.03	0.24	0.28	201
18HRCS-30	455	0.3	0.43	<0.01	2.27	0.03	0.22	1.29	596
18HRCS-32	455	0.7	1.25	<0.01	7.38	<0.02	0.74	3.7	84
18HRCS-35	163	1	0.74	<0.01	10.3	<0.02	0.57	4.17	12
18HRRT-03	478	0.3	0.39	0.03	0.46	0.02	0.23	0.25	620
18HRRT-05	57.6	0.2	0.19	0.01	0.78	<0.02	0.1	0.39	103
18HRRT-11	838	0.3	0.1	0.01	0.17	0.09	0.07	0.09	113
18HRKK-04	554	0.2	0.08	0.04	0.22	<0.02	0.04	0.13	61
18HRKK-07	167.5	1	0.94	0.01	6.87	<0.02	0.57	1.83	5
HR-1A	248	0.2	0.55	<0.01	0.36	0.05	0.3	0.37	288
HR-5C	316	0.7	0.93	<0.01	10.2	0.29	0.38	2.31	27
Analytical Method:	ME-MS81	ME-MS81	ME-MS81	ME-MS42	ME-MS81	ME-MS42	ME-MS81	ME-MS81	ME-MS81

Table 2 continued.

SAMPLE	W ppm	Y ppm	Yb ppm	Zn ppm	Zr ppm
HR-2G	<1	24.3	2.35	22	120
HR-3F	1	29.2	3.91	26	37
HR-4E	<1	18.3	1.68	92	39
HR-6GR	<1	44.9	5.14	13	332
18HRAC-02	1	5.5	0.57	62	14
18HRAC-08	1	6.7	0.94	101	58
18HRAC-10	1	24.7	4.23	32	234
18HRAC-15	1	3	0.47	18	4
18HRAC-16	2	10.4	1.3	12	24
18HRAC-18	1	27.9	3.55	72	135
18HRAC-19	1	13.7	1.5	122	36
18HRCS-02	3	6.1	0.66	65	24
18HRCS-08	1	0.9	0.13	15	5
18HRCS-14	1	9.1	1.11	51	81
18HRCS-18	1	28.2	4.32	39	461
18HRCS-22	5	47.4	5.1	35	425
18HRCS-24	1	11.6	1.47	51	172
18HRCS-29	1	12.6	1.63	106	32
18HRCS-30	2	13.3	1.63	81	56
18HRCS-32	2	39.9	4.85	116	175
18HRCS-35	1	20.1	4.27	13	419
18HRRT-03	1	14.3	1.74	91	24
18HRRT-05	1	6.8	0.82	105	30
18HRRT-11	11	3.5	0.47	47	7
18HRKK-04	1	2.6	0.3	83	12
18HRKK-07	1	29.3	4.15	53	385
HR-1A	1	19.7	2.03	88	46
HR-5C	<1	24.8	2.29	41	245
Analytical Method:	ME-MS81	ME-MS81	ME-MS81	ME-4ACD81	ME-MS81

GEOCHRONOLOGY

We would like to thank Dr. Kevin Chamberlain, Department of Geology and Geophysics, University of Wyoming, for processing and dating samples collected from the Horatio Rock quadrangle. These dates are crucial to understanding the timing of intrusive, metamorphic, and structural events, and also the lithological relationships within the quadrangle and the southern Medicine Bow Mountains.

Dr. Kevin Chamberlain analyzed four Horatio Rock samples for U-Pb radiometric dates using a chemical abrasion and thermal ionization mass spectrometry method (CA-TIMS). The following is a summary of Dr. Chamberlain's methods, results, and interpretations of his analyses.

Report to Wyoming State Geological Survey on CA-TIMS U-Pb zircon dating of magmatic rocks in the Horatio Rock quadrangle, southeast Wyoming

April 1, 2019. Kevin R. Chamberlain, Research Professor, Department of Geology and Geophysics, University of Wyoming

Methods

Zircon grains were separated by standard crushing and mineral separation methods. Selected zircons were annealed at 850°C for 50 hours, then dissolved in two steps in a chemical abrasion, thermal ionization mass spectrometric U-Pb dating method (CA-TIMS) modified from Mattinson (2005). The first dissolution step was in hydrofluoric acid (HF) and nitric acid (HNO_3) at 180°C for 12 hours. This removed the most metamict zircon domains in the annealed crystals. Individual grains were then spiked with a mixed ^{205}Pb-^{233}U-^{235}U tracer (ET535), completely dissolved in HF and HNO_3 at 240°C for 30 hours, and then converted to chlorides. The dissolutions were loaded onto rhenium filaments with phosphoric acid and silica gel without any further chemical processing. Pb and UO_2 isotopic compositions were determined in single Daly-photomultiplier mode on a Micromass Sector 54 mass spectrometer. Data were reduced and ages calculated using PbMacDat and ISOPLOT/EX after Ludwig (1988, 1991, 1998). The concordia age used in this report is a specific algorithm created by Ludwig (1998) to combine both $^{206}Pb/^{238}U$ and $^{207}Pb/^{235}U$ data from concordant analyses. Concordia ages reported here include the contributions from the U-decay constant uncertainties and can be compared to dates from other methods as long as those methods also propagate all sources of uncertainty.

Results

HR-2G: foliated granite (Xfg)

Zircons recovered from this sample were moderately sized (100–200 microns), iron stained, and extremely metamict (fig. 2). High-uranium zircons often exhibit radiation damage of the crystal lattice. Although the measured uranium concentrations are relatively low from the analyzed zircons (5–500 ppm, table 3), the Pb concentrations are greater than 10x those of HR-4E, and the data are reversely discordant due to uranium loss (table 3), which together suggest that the original uranium concentrations were several 1,000 ppm. Furthermore, the measured Th/U of these zircons is 8 to 27 (table 3), in part due to the U loss, but also indicating relatively higher thorium contents than in HR-6GR and HR-4E. The additional radiation damage from such high U and Th concentrations may be a factor for this sample. Common Pb is also quite high from these zircons even though chemical abrasion typically removes a significant amount of labile common Pb (Mattinson, 2005). The high common Pb may reflect incursion of Pb into the crystal lattice at some point in the zircons' histories. The U loss could have occurred naturally, although it is more common for Pb to be lost than for U. It is more likely that the uranium was disproportionately removed during the first partial dissolution step of the chemical abrasion process. Very few of the zircons survived that first step (fig. 2), and these survivors were small, ~50 μm deeply pitted domains, so it is conceivable that uranium was mobile during that step.

If the uranium loss is recent, either during uplift of the Medicine Bow Mountain Range or in the lab, and any potential incursion of Pb into the lattices occurred at a single time, then the Pb isotope data will preserve a reasonable date even without reliable uranium data. This is one of the strengths of the U-Pb system, its ability to preserve dates through some alteration and disturbance. Assuming that the U loss was recent, the $^{207}Pb/^{204}Pb$ versus $^{206}Pb/^{204}Pb$ date of 1,562.1±3.8 Ma (fig. 3, table 4) is interpreted as the magmatic age. This age is very close to that from a pegmatitic dike in the Woods Landing quadrangle (1,514±36 Ma, Campbell and Shelton, in press) and the zircon systematics, including extreme U loss characterized those zircons as well. This intrusion and the pegmatites may reflect the same magmatic event. Upper greenschist metamorphism associated with deformation has been documented as young as 1,550 Ma in the Sierra Madre and in the Medicine Bow mountains (Strickland, 2004; Duebendorfer and others, 2006; Sigler, 2008; Cubrich, 2017), including the Illinois Creek shear zone in the Horatio Rock quadrangle (Strickland, 2004). This new date suggests there was coeval magmatism during deformation. It also supports preliminary data from the Pinkham Granite ~6 km to the south (unpublished) for ca. 1,550 Ma magmatism.

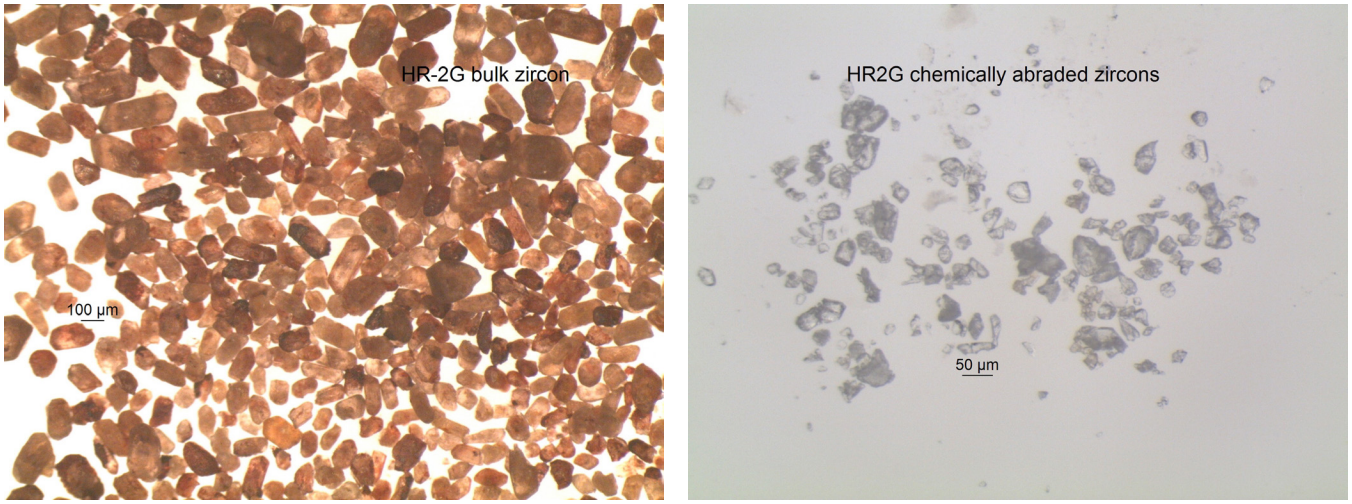

Figure 2. Examples of bulk zircons from HR-2G, selected for annealing and chemical abrasion ID-TIMS dating, upper, and the domains that survived the first, partial dissolution step of chemical abrasion, lower. Due to the small sizes of the surviving shards (note the left panel is double the magnification of the right panel), multi-grain picks were dissolved for U-Pb isotopic analyses and dating.

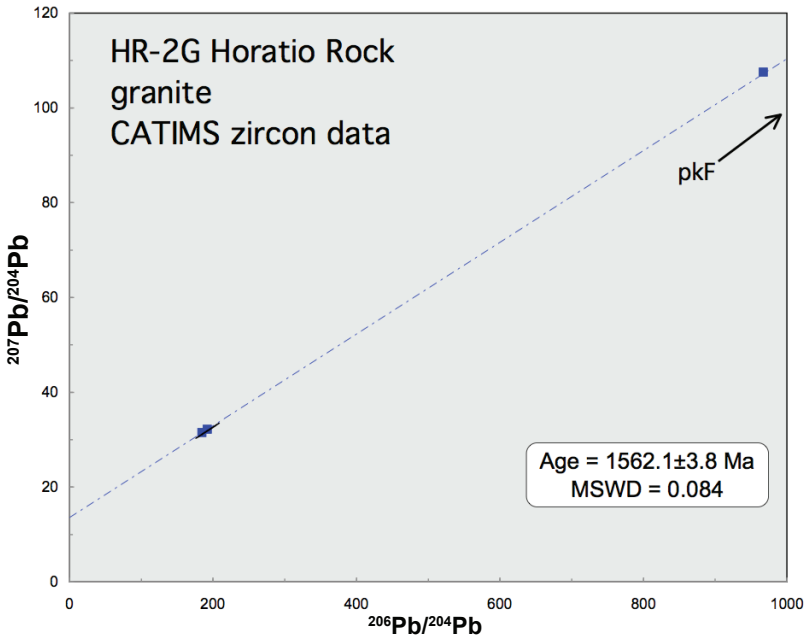

Figure 3. $^{207}Pb/^{204}Pb$ versus $^{206}Pb/^{204}Pb$ plot of CATIMS data from HR-2G. Assuming that the uranium loss is recent, whether geologic or in the laboratory, the Pb-Pb date will be an accurate date on magmatic growth of the zircons. Data points are augmented with blue squares as the ellipses are too small to see easily. The linear regression includes the three points shown plus one off scale.

HR-3F: small felsic intrusive (Xgfi)

Zircons recovered from this sample are mostly metamict and Fe stained (fig. 4). Like those from HR-2G, only small shards survived the first dissolution step of chemical abrasion and exhibit substantial U loss (reverse discordance of 98 to 141 percent, table 3). Unlike the HR-2G data, the $^{207}Pb/^{204}Pb$ versus $^{206}Pb/^{204}Pb$ results are nonlinear (MSWD=28, probability of fit is 0.000, fig. 5), so no Pb-Pb isochron is possible. The $^{207}Pb/^{206}Pb$ dates from two single shards and three multi-shard analyses range from 1,710 to 1,600 Ma (fig. 6), requiring multiple age components consistent with the nonlinearity of the Pb-Pb data. These results could reflect ≥1,710 Ma magmatism with variable metamorphic alterations ca. 1,550 Ma (≤1,600 Ma) or ca. 1,550 Ma magmatism with inherited cores at least as old as 1,710 Ma. Neither of these end-member interpretations is favored currently.

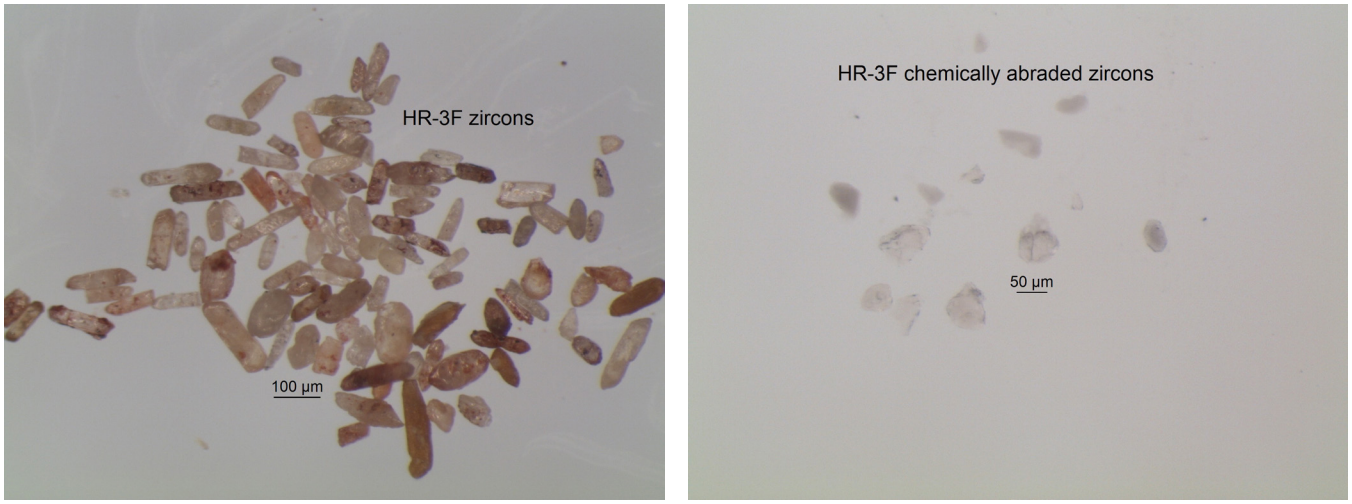

Figure 4. Bulk zircons recovered from HR-3F. Note Fe staining and very metamict natures. Only small shards survived the first step of chemical abrasion (note different magnification between panels).

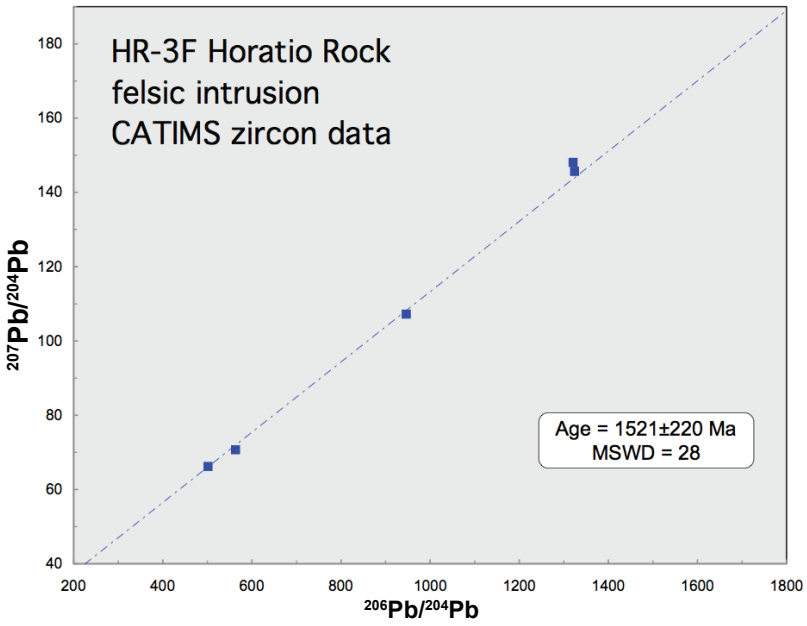

Figure 5. Total Pb data are non-linear on a Pb-Pb plot (MSWD = 28), indicating multiple age components.

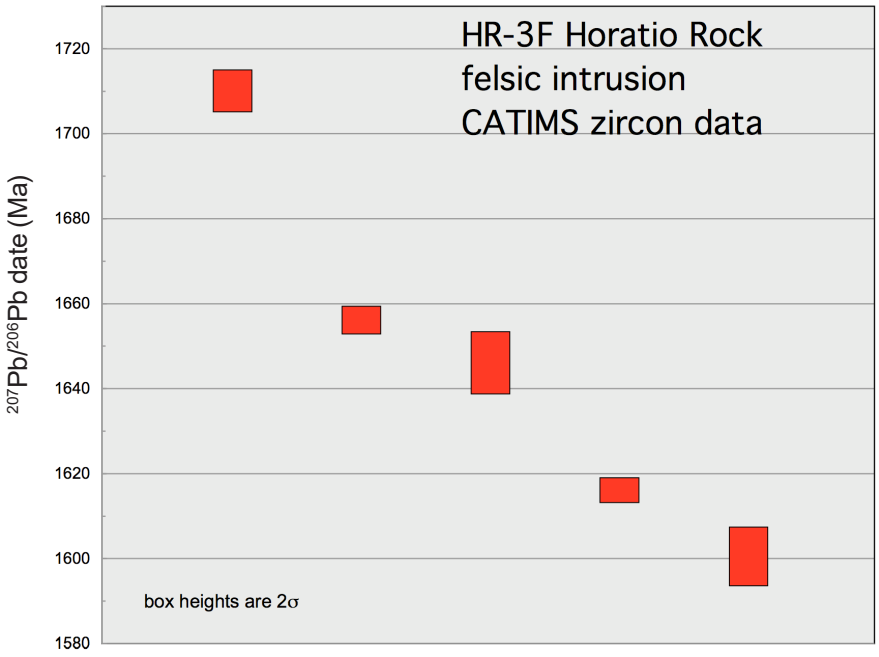

Figure 6. Analyses yielded an array of $^{207}Pb/^{206}Pb$ dates indicating multiple age components, consistent with non-linearity on a Pb-Pb plot (fig. 5).

HR-4E: diorite (Xd)

This rock is coarse grained with finer-grained mafic inclusions that may represent dismembered mafic dikes. The mafic enclaves were avoided during processing to ensure that the date relates to the dominant, more felsic portion. Zircons recovered from this sample were extra large, >200 microns in length with some fragments, suggesting grains as large as 1 mm must exist (fig. 7). They were relatively low in uranium concentrations, less than 200 ppm (table 3), and most survived the partial dissolution step as whole grains, albeit deeply eroded along crystal imperfections. Data from three single-grain analyses are concordant with a concordia age of 1,775.0±4.8 Ma (fig. 8) and weighted mean $^{207}Pb/^{206}Pb$ date of 1,775.1±1.8 Ma (fig. 9, table 3). The weighted mean date is interpreted as the best estimate of the magmatic age of this intrusion. Regionally, this age overlaps with that of the Mullen Creek mafic complex to the north within the Horatio Rock quadrangle, which has been dated to 1,778±2 Ma (Loucks and others, 1988) and with the Lake Owen layered mafic complex approximately 15 km to the northeast in the Albany quadrangle (1,775.1±3.0 Ma; Sutherland and Kragh, 2018). It is possible that this intrusion is related to either or both of these mafic complexes, perhaps as the feeder system or as dikes radiating from the complexes.

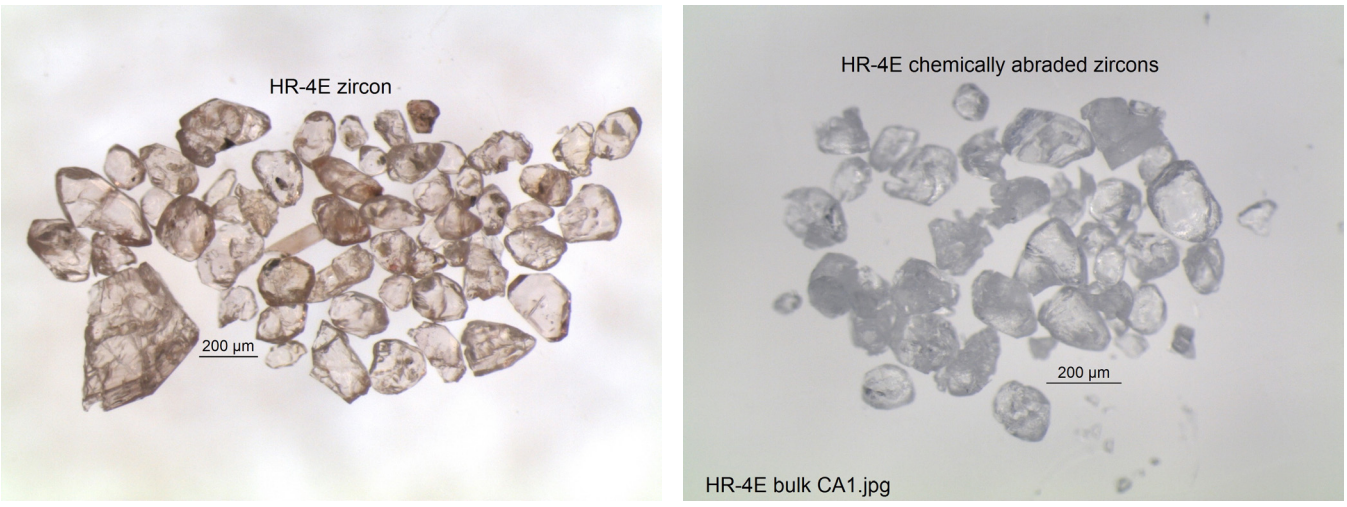

Figure 7. Zircons recovered from HR-4E. The grains were extra large, relatively free of defects and lacking discernable metamict zones (left panel). The first partial dissolution step of chemical abrasion followed grain defects (right panel), but left many large competent grains intact. These observations are consistent with low uranium concentrations, less than 200 ppm, and thus less crystal damage due to radiation.

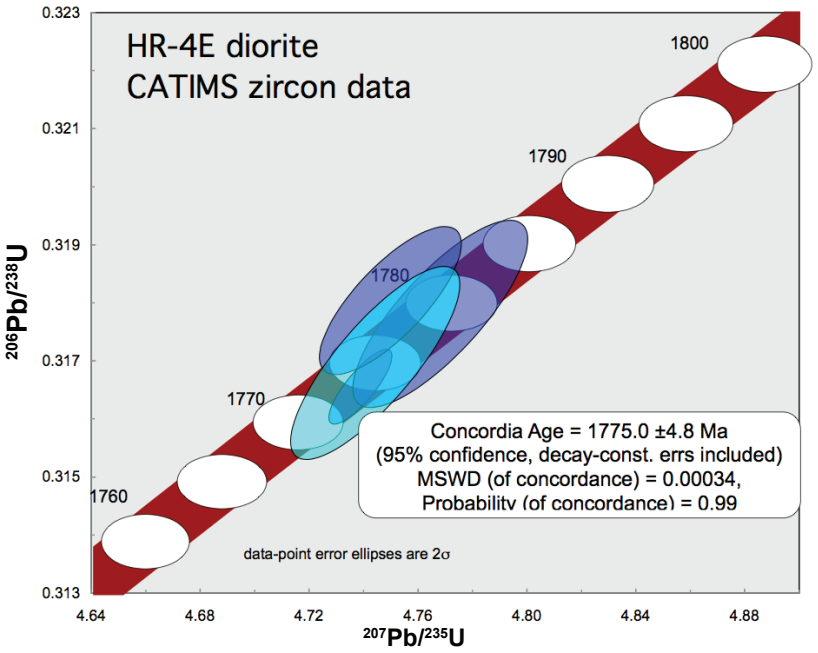

Figure 8. Concordia plot of four single zircon CATIMS analyses from HR-4E. Uncertainties in the U-decay constants are shown as a swath for the concordia curve. The three purple ellipses overlap each other and concordia and yielded a concordia age of 1,775.0±4.8 Ma (blue-green ellipse).

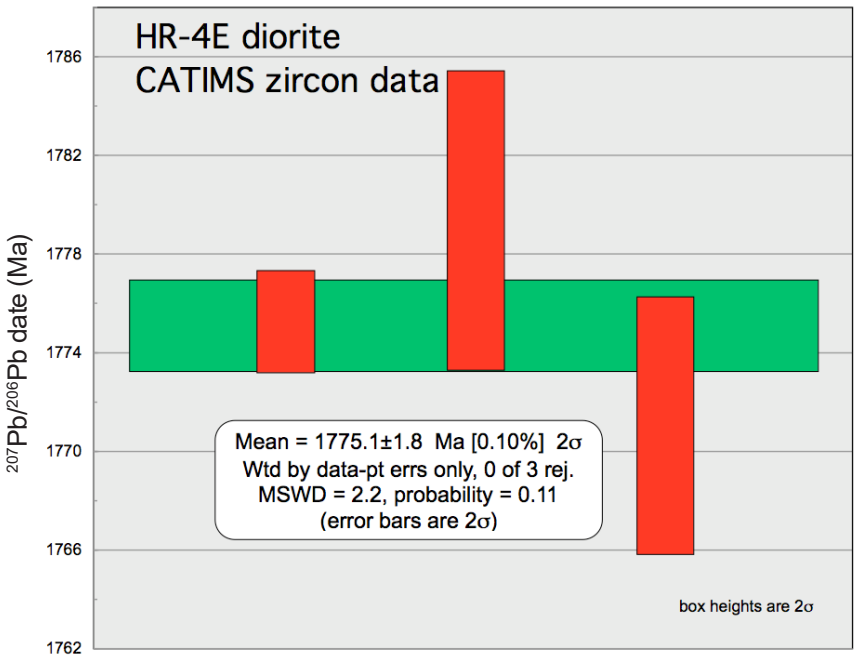

Figure 9. Plot of $^{207}Pb/^{206}Pb$ dates from three single-zircon, CATIMS analyses from HR-4E. The weighted mean date from the three concordant analyses (fig. 8) is interpreted as the best estimate of the magmatic age of the rock.

HR-6GR: foliated granite (Xfg)

Many of the zircons recovered from this sample were metamict (fig. 10), but competent domains survived the first partial dissolution step of chemical abrasion. The surviving domains were relatively small (<50 microns, fig. 10) and contained only trace amounts of Pb. A single shard and three multi-shard picks (two to five shards each) were dissolved for U-Pb isotopic analysis. Three of the analyses overlap each other on concordia and yield a concordia age (Ludwig, 1998) of 1,782.1±3.5 Ma (fig. 11), in good agreement with the weighted mean $^{207}Pb/^{206}Pb$ date of 1,785.0±1.9 Ma (fig. 12, table 3). The weighted mean $^{207}Pb/^{206}Pb$ date is interpreted as the best estimate of the magmatic age of this intrusion. This date overlaps the high-precision U-Pb date on the Keystone Quartz Diorite in the Woods Landing quadrangle to the east (1,784.7±1.9 Ma, Campbell and Shelton, in press), a biotite tonalite dated in

the Fox Park quadrangle (1,785.3±2.1 Ma, Carnes and others, in press) and several basement dates from the Green Mountain arc terrane in the Sierra Madre (Encampment River granodiorite, 1,779±5 Ma, Premo and Van Schmus 1989; and a bimodal metagabbro-granodiorite suite in the Big Creek region, 1,782±7 Ma and 1,777±11 Ma, Jones and others, 2010). In addition, HR-6GR is host to a distinctive intrusion of mafic dikes that were subsequently folded (fingerprint) in the southwestern portion of the Horatio Rock quadrangle, and the new date provides a maximum age of intrusion of those dikes.

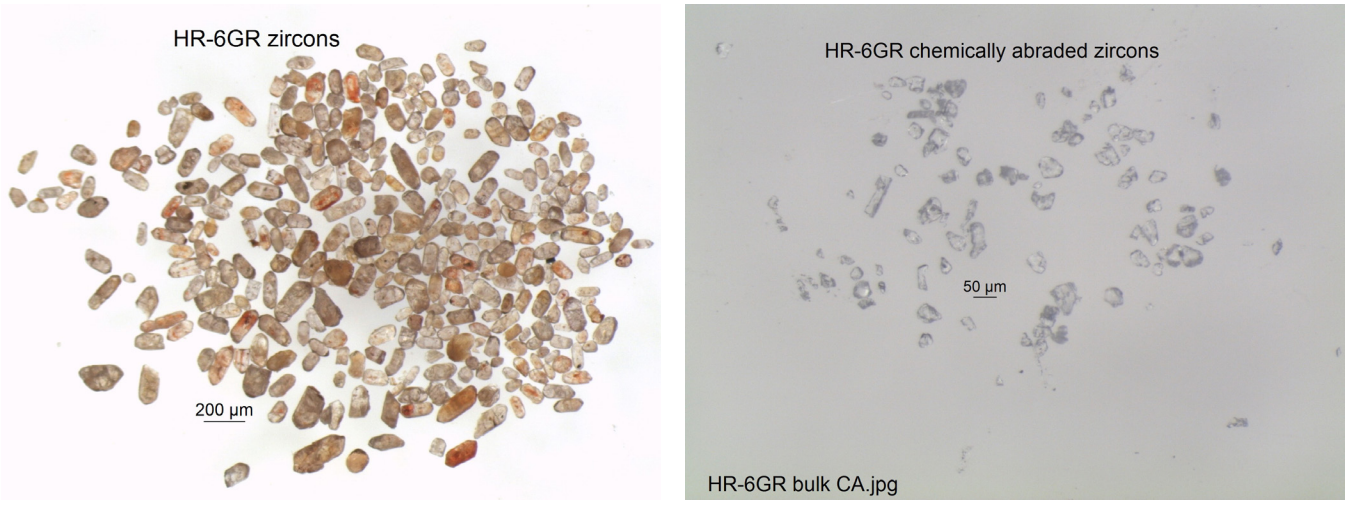

Figure 10. Examples of bulk zircons from HR-6GR, selected for annealing and chemical abrasion ID-TIMS dating (left panel), and the domains that survived the first, partial dissolution step of chemical abrasion (right panel). Individual shards were dissolved completely for U-Pb isotopic analyses and dating.

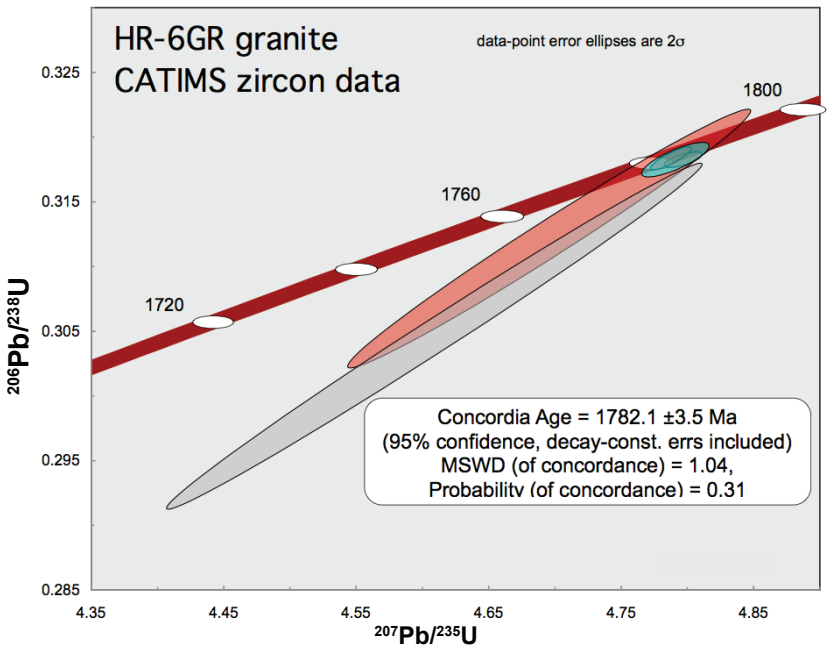

Figure 11. Concordia plot of four single zircon CATIMS analyses from HR-6GR. Uncertainties in the U-decay constants are shown as a swath for the concordia curve. The three red ellipses that overlap each other and concordia yielded a concordia age of 1,782.1±3.5 Ma (small green ellipse). The slightly discordant gray ellipse was not included in that calculation.

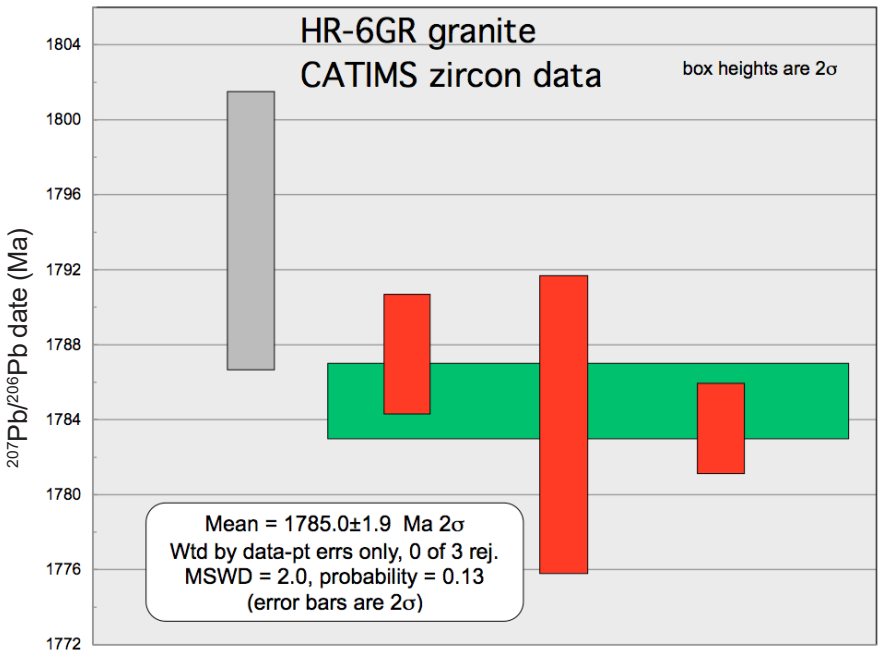

Figure 12. Plot of $^{207}Pb/^{206}Pb$ dates from four single-zircon, CATIMS analyses from HR-6GR. The weighted mean date from the three concordant analyses (fig. 11) is interpreted as the best estimate of the magmatic age of the rock.

Table 3. CATIMS (Chemical Abrasion, Thermal Ionization Mass Spectrometry) U-Pb zircon data. Significant digits as reported from Kevin Chamberlain.

								Corrected atomic ratios																
			sample Pb							$^{206}Pb/^{238}U$		$^{207}Pb/^{235}U$		$^{207}Pb/^{206}Pb$		206/238	207/235	207/206				Weighted mean		Number
Sample	Weight (µg)	U (ppm)	(ppm)	(pg)	cPb (pg)	Pb*/Pbc	Th/U	$^{206}Pb/^{204}Pb$	$^{208}Pb/^{206}Pb$	(rad.)	%err	(rad.)	%err	(rad.)	%err	Age (Ma)	Age (Ma)	Age (Ma)	err	Rho	% disc.	$^{207}Pb/^{206}Pb$ date	2 sigma MSWD	of Points
HR-2G																								
sA	0.68	5.1	17.5	12	6	2.0	8.3	127	0.237	2.845	(3.29)	38.04	(3.86)	.0970	(2.03)	8,682.2	3,720.9	1,566.5	± 38	0.85	-934	See Table 4, no resolvable date from U-Pb data, extreme U loss		
pkD 5g	0.30	58	526	160	41	3.0	18.0	172	0.236	6.098	(2.10)	80.75	(2.18)	.0960	(0.55)	12,633.8	4,471.4	1,548.5	± 10	0.97	-2,146			
pkF 5g	0.11	30	74	8	5	1.7	6.7	111	0.258	2.104	(0.78)	28.06	(3.24)	.0967	(2.84)	7,300.8	3,421.1	1,562.1	± 53	0.60	-667			
pkE 5g	0.30	544	7,627	2,317	540	3.3	27.9	183	0.238	9.386	(0.73)	124.14	(0.90)	.0959	(0.48)	15,087.8	4,903.7	1,546.2	± 9	0.84	-3,363			
HR-3F																								
sC	4.32	197	1,121	4,843	67	71	65.3	468	9.56	0.607	(0.63)	8.77	(0.68)	.1047	(0.24)	3,057.9	2,314.0	1,709.9	± 4.4	0.93	-100	Range of 207Pb/206Pb dates, no resolvable date from U-Pb or Pb-Pb data, extreme U loss		
pkF 3g	1.71	414.9	2,017	3,450	27	125	55.8	1,098	6.79	0.706	(5.24)	9.91	(5.24)	.1017	(0.17)	3,445.2	2,426.6	1,656.2	± 3.2	1.00	-141			
pkE 3g	1.71	174.1	829	1,420	24	58	55.6	458	7.82	0.607	(0.79)	8.47	(0.89)	.1012	(0.38)	3,057.8	2,282.6	1,646.2	± 7.0	0.90	-109			
sB	2.36	290	1,442	3,403	22	153	60.7	1,048	9.03	0.564	(3.80)	7.74	(3.80)	.0996	(0.15)	2,881.8	2,201.2	1,616.3	± 2.8	1.00	-98			
pkD 2g	1.28	210	1,492	1,909	16	122	89.9	665	11.86	0.629	(1.34)	8.57	(1.40)	.0988	(0.36)	3,147.5	2,293.5	1,600.7	± 6.8	0.97	-123			
HR-4E																						1775.1±1.8 Ma	2.2	3
sB	15.2	79	26	397	10.5	37	0.27	2,231	0.078	0.3181	(0.33)	4.7495	(0.45)	0.1083	(0.29)	1,780.2	1,776.0	1,771.1	± 5.2	0.77	-0.59			
sE	4.5	107	34	155	4.6	33	0.24	2,088	0.071	0.3178	(0.41)	4.7677	(0.55)	0.1088	(0.33)	1,779.1	1,779.2	1,779.4	± 6.1	0.80	0.02			
sC	13.5	185	60	806	2.9	277	0.26	17,154	0.076	0.3166	(0.16)	4.7383	(0.20)	0.1086	(0.11)	1,773.0	1,774.0	1,775.3	± 2.1	0.82	0.15			
HR-6GR																						1785.0 ±1.9 Ma	2.0	3
pkF 5g	0.18	2,075	676	122	0.5	238	0.28	14,690	0.080	0.3184	(0.23)	4.7868	(0.26)	0.1090	(0.13)	1,781.7	1,782.6	1,783.6	±2.4	0.87	0.12			
pkE 3g	0.68	266	87	58	2.0	29.9	0.27	1,862	0.079	0.3183	(0.15)	4.7960	(0.24)	0.1093	(0.17)	1,781.3	1,784.2	1,787.5	±3.2	0.69	0.40			
sC	0.20	369	117	24	1.6	14.5	0.24	921	0.070	0.3122	(2.60)	4.6948	(2.65)	0.1091	(0.43)	1,751.6	1,766.3	1,783.8	±7.9	0.99	2.06			
pkD 2g*	1.69	54	17	29	2.4	12.0	0.24	762	0.073	0.3047	(3.56)	4.6082	(3.59)	0.1097	(0.41)	1,714.7	1,750.8	1,794.1	±7.4	0.99	5.04			

Notes: sample: s_=single grain; pk_= multiple shards, _g=number of shards, * excluded from calculation.

Weight: represents estimated weight after first step of CATIMS zircon dissolution and is only approximate. U and Pb concentrations are based on this weight and are useful for internal comparisons only. Picograms (pg) sample and common Pb from the second dissolution step are measured directly however, and are accurate.

sample Pb: sample Pb (radiogenic + initial) corrected for laboratory blank

cPb: total common Pb. All was assigned to laboratory blank.

Pb*/Pbc: radiogenic Pb to total common Pb (blank + initial)

Th/U based on measured $^{208}Pb/^{206}Pb$ value and $^{207}Pb/^{206}Pb$ date. It reflects initial conditions if U loss was recent.

Corrected atomic ratios: $^{206}Pb/^{204}Pb$ corrected for mass discrimination and tracer, all others corrected for blank, mass discrimination, tracer and initial Pb, values in parentheses are 2 sigma errors in percent.

Rho: $^{206}Pb/^{238}U$ vs $^{207}Pb/^{235}U$ error correlation coefficient

% disc: percent discordant, - is reversely discordant

Zircon dissolution and chemistry were adapted from methods developed by Krogh (1973), Parrish et al. (1987) and Mattinson (2005). All zircons were chemically abraded (CATIMS). Final dissolutions were spiked with a mixed $^{205}Pb/^{233}U/^{235}U$ tracer (ET535). Pb and UO2 from zircons were loaded onto single rhenium filaments with silica gel without any ion exchange cleanup; isotopic compositions were measured in single Daly-photomultiplier mode on a Micromass Sector 54 thermal ionization mass spectrometer at the University of Wyoming. Mass discrimination for Pb was 0.245±0.10 %/amu for Daly analyses based on replicate analyses of NIST SRM 981.

U fractionation was determined internally during each run. Measured procedural blanks ranged from 2 to 0.38 pg Pb during the course of the study. U blanks were consistently less than 0.1 pg. Isotopic composition of the Pb blank was measured as 18.649±0.403, 15.540±0.48, and 37.804±1.69 for 206/204, 207/204 and 208/204, respectively. Concordia coordinates, intercepts, uncertainties and Cooncrdia Ages were calculated using PBMacDAT and ISOPLOT programs (based on Ludwig 1988, 1991, 1998); $^{206}Pb/^{238}U$ and $^{207}Pb/^{206}Pb$ ratios and dates corrected for Th disequilibrium assuming Th/U magma of 2.2 following Schärer (1984).

The decay constants used by PBMacDAT are those recommended by the I.U.G.S. Subcommission on Geochronology (Steiger and Jäger, 1977): 0.155125 x 10-9/yr for 238U, 0.98485 x 10-9/yr for ^{235}U and present-day $^{238}U/^{235}U = 137.88$.

Table 4. CATIMS (Chemical Abrasion, Thermal Ionization Mass Spectrometry) Pb-Pb zircon data. Significant digits as reported from Kevin Chamberlain.

				$^{206}Pb/^{204}Pb$		$^{207}Pb/^{204}Pb$						
Sample	Wt (µg)	U (ppm)	Pb (ppm)	Corr. Ratio	%err	Corr. Ratio	%err	Rho 6/4-7/4	Pb-Pb isochron date	MSWD	Number of points	Probability of fit
HR-2G									1562.1±3.8 Ma	0.089	4	
sA	0.68	5	17	967.03	(460)	107.55	(401)	1.000				
pkD 5g	0.30	58	526	191.75	(7.01)	32.21	(4.05)	0.998				
pkF 5g	0.11	30	74	139115	(0.71)	13471	(0.76)	0.963				
pkE 5g	0.30	544	7627	184.41	(0.55)	31.49	(0.46)	0.910				
HR-3F									*non-linear*	28		0.000
sC	4.32	197	1121	501.47	(4)	66.19	(3)	0.998				
pkF 3g	1.71	415	2017	1320.62	(12)	148.08	(11)	1.000				
pkE 3g	1.71	174	829	562.86	(14)	70.68	(11)	1.000				
sB	2.36	290	1442	1324.43	(16)	145.63	(14)	1.000				
pkD 2g	1.28	210	1492	946.57	(26)	107.23	(22)	1.000				

Notes: sample: s_=single grain; pk_= multiple shards, _g=number of shards.

Weight: weight estimated after first step of CATIMS zircon dissolution. Corrected atomic ratios: corrected for mass discrimination and tracer, values in parentheses are 2 sigma errors in percent.

Rho: $^{206}Pb/^{204}Pb$ vs $^{207}Pb/^{204}Pb$ error correlation coefficient

REFERENCES

Campbell, E.A., and Shelton, C.R., in press, Preliminary geologic map of the Woods Landing quadrangle, Albany County, Wyoming: Wyoming State Geological Survey Open File Report 2018-3, scale 1:24,000.

Carnes, J.D., Chumley, A.S., and Samra, C.P., in press, Preliminary geologic map of the Foxpark quadrangle, Albany County, Wyoming: Wyoming State Geological Survey Open File Report 2018-2, scale 1:24,000.

Condie, K.C., 1982, Plate-tectonics model for Proterozoic continental accretion in the southwestern United States: Geology, v. 10, p. 37–42.

Cubrich, B.T., 2017, Paleoproterozoic history of the Rocky Mountains—Using using multiple geochronologic methods to unravel the Proterozoic structural history of polyphase deformation in highly deformed rocks: Laramie, University of Wyoming, M.S. thesis, 444 p., 5 pls.

Duebendorfer, E.M., 1986, Structure, metamorphism, and kinematic history of the Cheyenne belt, Medicine Bow Mountains, southeastern Wyoming: Laramie, University of Wyoming, PhD dissertation, 323 p., scale 1:24,000 and 1:50,000.

Duebendorfer, E.M., Chamberlain, K.R., and Heizler, M., 2006, Filling the North American Proterozoic tectonic gap—1.60-1.59-Ga deformation and orogenesis in Southern Wyoming, USA: Journal of Geology, v. 114, no. 1, p. 19–42.

Duebendorfer, E.M., 1986, Structure, metamorphism, and kinematic history of the Cheyenne belt, Medicine Bow Mountains, southeastern Wyoming(unpublished): Laramie, University of Wyoming, PhD dissertation, 323 p., map scale 1:24,000.

Duebendorfer, E.M., and Houston, R.S., 1987, Proterozoic accretionary tectonics at the southern margin of the Archean Wyoming craton: Geological Society of America Bulletin, v. 98, p. 554–568.

Hausel, W.D., 1997, Copper, lead, zinc, molybdenum, and associated metal deposits of Wyoming: Wyoming State Geological Survey Bulletin 70, 229 p., 15 pls.

Houston, R.S., McCallum, M.E., King, J.S., Ruehr, B.B., Myers, W.G., Orback, C.J., King, J.R., Childers, M.O., Irwin Matus, Currey, D.R., Gries, J.C., Stensrud, H.L., Catanzaro, E.J., Swetnam, M.N., Michalek, D.D., and Blackstone, D.L., Jr., 1968, A regional study of rocks of Precambrian age in that part of the Medicine Bow Mountains lying in southeastern Wyoming—With a chapter on the relationship between Precambrian and Laramide structure: Geological Survey of Wyoming [Wyoming State Geological Survey] Memoir 1, 167 p., 35 pls. (Reprinted Reprinted 1978.)

Jones, D.S., Snoke, A.W., Premo, W.R., and Chamberlain, K.R., 2010, New models for Paleoproterozoic orogenesis in the Cheyenne belt region—Evidence evidence from the geology and U-Pb geochronology of the Big Creek Gneiss southeastern Wyoming: Geological Society of America Bulletin, v. 122, no. 11–12, p. 1,877–1,898.

Krogh, T.E., 1973, A low-contamination method for hydrothermal decomposition of zircon and extraction of U and Pb for isotopic age determinations: Geochimica et Cosmochimica Acta, v. 37, p. 485–494.

Loucks, R.R., Premo, W.R., and Snyder, G.L., 1988. Petrology, structure, and age of the Mullen Creek layered mafic complex and age of arc accretion, Medicine Bow Mountains, Wyoming: Geological Society of America Abstracts with Programs, no. 20, p. A73.

Ludwig, K.R., 1988, PBDAT for MS-DOS, a computer program for IBM-PC compatibles for processing raw Pb-U-Th isotope data, version 1.24: U.S. Geological Survey Open -File Report 88-542, 32 p.

Ludwig, K.R., 1991, ISOPLOT for MS-DOS, a plotting and regression program for radiogenic-isotope data, for IBM-PC compatible computers, version 2.75: U.S. Geological Survey Open -File Report 91-445, 45 p.

Ludwig, K.R., 1998, On the treatment of concordant uranium-lead ages: Geochimica et Cosmochimica Acta, v. 62, no. 4, p. 665–676.

Mattinson, J.M, 2005, Zircon U-Pb chemical abrasion ("CA-TIMS") method—Combined combined annealing and multi-step partial dissolution analysis for improved precision and accuracy of zircon ages: Chemical Geology, v. 220, p. 47–66.

Myers, W.G., 1958, Geology of the Sixmile Gap area, Albany and Carbon counties, Wyoming: Laramie, University of Wyoming, M.S. thesis, 74 p., 3 pls.

Parrish, R.R., Roddick, J.C., Loveridge, W.D., and Sullivan, R.D., l987, Uranium-lead analytical techniques at the geochronology laboratory, Geological Survey of Canada, in Radiogenic age and isotopic studies, Report 1: Geological Survey of Canada Paper 87-2, p. 3–7.

Premo, W.R., and Loucks, R.R., 2000, Age and Pb-Sr-Nd isotopic systematics of plutonic rocks from the Green Mountain magmatic arc, southeastern Wyoming—Isotopic isotopic characterization of a Paleoproterozoic island arc system: Rocky Mountain Geology, v. 35, no. 1, p. 51–70.

Premo, W.R., and Van Schmus, W.R., 1989, Zircon geochronology of Precambrian rocks in southeastern Wyoming and northern Colorado, in Grambling, J.A, and Tewksbury, B.J., eds., Proterozoic geology of the Southern Rocky Mountains: Geological Society of America Special Paper 235, p. 13–32.

Ruehr, B.B., 1961, Geology of Devils Gate area, Albany and Carbon counties, Wyoming: Laramie, University of Wyoming, M.S. thesis, 48 p., 1 pl., scale 1:24,000.

Sigler, J.T., 2008, The metamorphic and structural evolution of the Davis Peak area, northern Park Range, Colorado: Laramie, University of Wyoming, M.S. thesis, 259 p., 1 pl., scale 1:24,000.

Stacey, J.S. and Kramers, J.D., 1975, Approximation of terrestrial lead isotope evolution by a two-stage model: Earth and Planetary Science Letters, v. 26, p. 207–221.

Steiger, R.H., and Jäger, Emilie., 1977, Subcommission on geochronology—Convention on the use of decay constants in geo- and cosmochronology: Earth and Planetary Science Letters, v. 36, p. 359–362.

Strickland, D.S., 2004, Structural and geochronologic evidence for the Ca. 1.6 Ga reactivation of the Cheyenne belt, southeastern Wyoming: Laramie, University of Wyoming, M.S. thesis, 157 p.

Sutherland, W.M., and Hausel, W.D., 2004, Preliminary geologic map of the Saratoga 30' x 60' quadrangle, Carbon and Albany counties, Wyoming: Wyoming State Geological Survey Open File Report 04-10, 34 p., 1 pl., scale 1:100,000.

Sutherland, W.M., and Hausel, W.D., 2005, Preliminary geologic map of the Keystone quadrangle, Albany and Carbon counties, Wyoming: Wyoming State Geological Survey Open File Report 05-6, 21 p., 1 pl., scale 1:24,000.

Sutherland, W.M., Stafford, J.E., Carroll, C.J., Gregory, R.W., and Kehoe, K.S., 2018, Mines and minerals map of Wyoming: Wyoming State Geological Survey, accessed September 2018, at http://wsgs.maps.arcgis.com/apps/webappviewer/index.html?id=af948a51f4954a81adeae8935440cd28.

Swetnam, M.N., 1961, Geology of the Pelton Creek area, Albany and Carbon counties, Wyoming: Laramie, University of Wyoming, M.S. thesis, 78 p., 13 pls., scale 1:15,500.

Whitmeyer, S.J., and Karlstrom, K.E., 2007, Tectonic model for Proterozoic growth of North America: Geosphere, v. 3, no. 4, p. 220–259.